

Low baseline pulmonary levels of cytotoxic lymphocytes as a predisposing risk factor for severe COVID-19

Pascal H.G. Duijf^{1,2,3*}

¹ Institute of Health and Biomedical Innovation, Queensland University of Technology (QUT), Faculty of Health, School of Biomedical Sciences, Brisbane QLD, Australia.

² Centre for Data Science, Queensland University of Technology (QUT), Brisbane QLD, Australia.

³ University of Queensland Diamantina Institute, The University of Queensland, Translational Research Institute, Brisbane QLD, Australia.

* Correspondence: Pascal H.G. Duijf, email: pascal.duijf@qut.edu.au

Abstract

COVID-19 is caused by the coronavirus SARS-CoV-2 and currently has detrimental human health, community and economic impacts around the world. It is unclear why some SARS-CoV-2-positive individuals remain asymptomatic, while others develop severe symptoms. Baseline pulmonary levels of anti-viral leukocytes, already residing in the lung prior to infection, may orchestrate an effective early immune response and prevent severe symptoms. Using "*in silico* flow cytometry", we deconvoluted the levels of all seven types of anti-viral leukocytes in 1,927 human lung tissues. Baseline levels of CD8⁺ T cells, resting NK cells and activated NK cells, as well as cytokines that recruit these, are significantly lower in lung tissues with high expression of the SARS-CoV-2 entry receptor ACE2. We observe this in univariate analyses, in multivariate analyses, and in two independent datasets. Relevantly, ACE2 mRNA and protein levels very strongly correlate in human cells and tissues. Above findings also largely apply to the SARS-CoV-2 entry protease TMPRSS2. Both SARS-CoV-2-infected lung cells and COVID-19 lung tissues show upregulation of CD8⁺ T cell- and NK cell-recruiting cytokines. Moreover, tissue-resident CD8⁺ T cells and inflammatory NK cells are significantly more abundant in bronchoalveolar lavages from mildly affected COVID-19 patients, compared to severe cases. This suggests that these lymphocytes are important for preventing severe symptoms. Elevated ACE2 expression increases sensitivity to coronavirus infection. Thus, our results suggest that some individuals may be exceedingly susceptible to develop severe COVID-19 due to concomitant high pre-existing ACE2 and TMPRSS expression and low baseline cytotoxic lymphocyte levels in the lung.

Keywords: COVID-19, SARS-CoV-2, ACE2, TMPRSS2, T cells, NK cells

Introduction

Coronaviruses are viruses belonging to the family of *Coronaviridae* (1). They are large, single-stranded RNA viruses that often originate from bats and commonly infect mammals. While the majority of coronavirus infections cause mild symptoms, some can cause severe symptoms, such as pneumonia, respiratory failure and sepsis, which may lead to death (2, 3).

Coronavirus zoonosis constitutes a serious health risk for humans. Indeed, in recent history, transmissions of three types of coronaviruses to humans have led to varying numbers of deaths. The outbreak of the Severe Acute Respiratory Syndrome (SARS) epidemic, which is caused by the SARS coronavirus (SARS-CoV), originated in Guangdong, China in 2002 and led to nearly 800 deaths (4). The Middle East Respiratory Syndrome coronavirus (MERS-CoV) outbreak, which emerged in Saudi Arabia in 2012, similarly caused about 800 deaths, although with over 8,000 cases, nearly four times as many cases were reported (4). Finally, Coronavirus Disease 19 (COVID-19), caused by Severe Acute Respiratory Syndrome Coronavirus 2 (SARS-CoV-2), is currently causing a pandemic. On 1 May 2020, the World Health Organization reported over 3 million confirmed cases and over 220,000 patients to have succumbed to COVID-19 around the world (5). However, the factual number of deaths is probably considerably higher (6). In addition, this figure is still soaring, on 1 May 2020 at a rate exceeding 6,400 deaths per day (5).

To infect target cells, coronaviruses use their spike (S) glycoprotein to bind to receptor molecules on the host cell membrane. Angiotensin-converting enzyme 2 (ACE2) has been identified as the main SARS-CoV-2 entry receptor on human cells (7, 8), while the serine protease TMPRSS2, or potentially cathepsin B and L, are used for S-protein priming to facilitate host cell entry (7). SARS-CoV-2 S-protein has a 10 to 20-fold higher affinity to human ACE2 than SARS-CoV S-protein (9). Moreover, ACE2 expression proportionally increases the susceptibility to S protein-mediated coronavirus infection (10-12). Hence, increased expression of ACE2 is thought to increase susceptibility to COVID-19 (13-15).

Epithelial cells of the respiratory tract, including the lung, are primary SARS-CoV-2 target cells (16-18). These cells can sense viral infection via pattern recognition receptors (PRRs). PRRs, including Toll-like receptors and NOD-like receptors, recognize pathogen-associated molecular patterns (PAMPs) (19). Upon PRR activation, a range of pro-inflammatory cytokines and chemokines are produced and released in order to activate the host's immune system. Interferons (IFNs), in particular type I and type III IFN, are among the principal cytokines to recruit immune cells (19, 20).

Six types of leukocytes have been implicated in detecting and responding to viral infections in the lung, a major site of SARS-CoV-2 infection, which also presents with severe COVID-19 symptoms. The cytotoxic activities of CD8+ T cells and NK cells can facilitate early control of viral infections by clearing infected cells and avoiding additional viral dissemination (21, 22). Dendritic cells specialize in sensing infections, including by viruses, and inducing an immune response (23). CD4+ T cells contribute to viral clearance by promoting production of cytokines and interactions between CD8+ T cells and dendritic cells (24). M1 macrophages interact with pulmonary epithelial cells to fight viral infections in the lung (25). Finally, neutrophils may contribute to clearance of viral infections through phagocytosis of virions and viral particles. However, their precise role is uncertain (26).

SARS-CoV-2 is considerably more efficient in infection, replication and production of infectious virus particles in human lung tissue than SARS-CoV (17). Strikingly, despite this, SARS-CoV-2 initially does not significantly induce type I, II or III IFNs in infected human lung cells and tissue (17, 27). When this does occur, it may in fact promote further SARS-CoV-2 infection, as IFNs directly upregulate expression of the SARS-CoV-2 receptor ACE2 (28). These observations suggest that baseline levels of leukocytes, which already reside in the lung prior to infection, may be important in mounting a rapid immune response against SARS-CoV-2 infection and prevent severe COVID-19 symptoms. As stated above, ACE2 expression level may be a predictor of increased susceptibility to COVID-19 (10-15)}. Thus, we here investigated the relationship between ACE2 and TMPRSS2 expression and the levels of seven leukocyte types implicated in anti-viral immune response in human lung tissue.

Results

We used bulk RNAseq gene expression data from the 578 human lung tissues present in the Genotype-Tissue Expression (GTEx) database (29, 30), because this is the largest publicly available dataset with clinical information. Using an established “*in silico* flow cytometry” pipeline (31), we estimated the levels of CD8+ T cells, resting and activated NK cells, M1 macrophages, dendritic cells, CD4+ T cells and neutrophils in these tissues (**Fig. S1a-c, Table S1**). We compared these to ACE2 expression levels in these lung tissues. This revealed that ACE2 expression is negatively correlated with the levels of CD8+ T cells, resting and activated NK cells and M1 macrophages ($p < 8 \times 10^{-6}$, Pearson correlations) (**Fig. 1a-c**). However, there are no statistically significant correlations between ACE2 expression and the levels of CD4+ T cells, dendritic cells and neutrophils ($p > 0.05$) (**Fig. S2a-d**). Thus, the levels of a majority of leukocytes involved in anti-viral immune responses are significantly lower in lung tissues with high ACE2 expression levels.

It is possible that some of above observations are linked to phenotypic characteristics, such as sex, age, body mass index (BMI), race or smoking status. To test the robustness of our findings, we applied multivariable regression analysis that includes these five covariates (**Table S2**), as well as the levels of the seven above leukocyte types or states. This showed that only 4 of the 12 variables significantly contribute to predicting ACE2 expression levels, specifically the levels of CD8+ T cells, resting NK cells, activated NK cells and M1 macrophages (**Fig. 1a-c, Table S3**). Notably, none of the five added phenotypic covariates showed statistically significant contributions. Consistently, we found limited statistically significant correlations between these variables and ACE2 expression in univariate analyses, irrespective of whether they were analyzed as continuous data or binned into discrete ordinal categories (**Fig. S4a-j**). Thus, the levels of four types of leukocytes that respond to viral infection are low in lung tissue with high ACE2 expression levels independently of phenotypic covariates.

Next, we tested whether above observations could be validated in an independent cohort of individuals. For this, we used the, to our knowledge, largest publicly available lung tissue dataset. The Laval University, University of British-Columbia, Groningen University (LUG) dataset includes microarray gene expression data of 1,349 human lung tissues. Following determination of ACE2

expression levels and estimation of the levels of CD8+ T cells, resting NK cells, activated NK cells and M1 macrophages (**Fig. S1a-c, Table S1**), we found that three of the four also negatively correlated with ACE2 expression in this independent dataset ($p < 2 \times 10^{-8}$) (**Fig. 1d-f**). With a correlation coefficient of $R = 0.096$, only M1 macrophages did not correlate with ACE2 expression in this dataset (**Fig. S3**). Thus, our observations indicate that the baseline levels of three types of cytotoxic lymphocytes, specifically CD8+ T cells, resting NK cells and activated NK cells, are robustly and consistently low in lung tissue with high expression of the SARS-CoV-2 receptor ACE2.

To more rigorously assess our observations, we employed a range of additional analyses. Although highly statistically significant (all p values $< 4.1 \times 10^{-6}$, **Fig. 1**), the absolute Pearson R values between baseline levels of ACE2 and the three lymphocyte types were seemingly low, as they ranged between 0.2 and 0.3 (**Fig 1a-c**). To test how strong these are in relative terms, we calculated the Pearson R and p values of 1000 randomly sampled other genes. This revealed that the ACE2 R and p values were significantly lower than expected by chance (all one-sample t test $p < 2.2 \times 10^{-16}$; **Fig 2a,b**). In addition, these R and p values ranked in the top 0.4 to 11 percentiles of strongest and most significant correlations for each of the three leukocyte types (**Fig 2a,b**). Thus, the seemingly low correlations between ACE2 mRNA and cytotoxic lymphocyte levels in the lung are not only highly statistically significant, but also strong in relative terms.

Further, we tested how well ACE2 mRNA and protein levels correlate. Using the mRNA and protein levels in 52 cell lines, we find that ACE2 mRNA levels strongly correlate with ACE2 protein levels in human cells (Pearson $R = 0.8155$, $p = 1.8 \times 10^{-13}$; **Fig. 2c**). In fact, ACE2 ranks in the top 1.8 percentile of over 12,000 genes with the strongest mRNA-protein level correlations ($p < 2.2 \times 10^{-16}$; **Fig 2d**). Using two ACE2-specific antibodies, immunohistochemistry on 40 human tissues also shows a strong ACE2 mRNA-protein correlation ($p = 0.0011$, Kruskal-Wallis test; **Fig. 2e**) and this is additionally validated by a meta-analysis that we conducted using nine published studies (Pearson $R = 0.7130$, $p = 0.0013$; **Fig. 2f, Table S4**). Therefore, we conclude that ACE2 mRNA and protein levels very strongly correlate, both in human cells and in human tissues.

Above, we found that baseline ACE2 levels in the lung negatively correlate with CD8+ T cells and resting and activated NK cells in multivariate analyses and in an independent dataset (**Fig. 1a-f**). Several cytokines, including CCL2-5, CXCL9, CXCL10, CXCL16 and IL18, are known to chemotactically attract CD8+ T cells and NK cells (32-37). Consistently, we find that the baseline levels of these chemokines in human lung tissue typically significantly correlate with the baseline levels of CD8+ T cells and resting and activated NK cells (**Fig. 2g, Fig. S5**). Additionally, as expected given our above results, we find significant negative correlations between the levels of ACE2 and the levels of six of these eight cytokines in the lung (**Fig. 2h**). These findings lend further support to our previous observations, suggesting that high levels of said cytokines in the lung establish a favorable milieu for cytotoxic lymphocytes, which correlates with low ACE2 levels.

Next, we assessed the direct consequences of SARS-CoV-2 infection. *In vitro* SARS-CoV-2 infection of human lung cells invariably leads to upregulation of all eight abovementioned CD8+ T cell- and NK cell-attracting cytokines, with six of these increases showing statistical significance (**Fig. 2i**). Similarly, compared to control lung tissues, all eight cytokines are upregulated in lung tissues from COVID-19 patients, with five showing statistical significance (**Fig. 2j**). Moreover, the levels of CD8+ T cells and NK cells are higher in bronchoalveolar lavages of mildly affected COVID-19 patients than in severe cases, with CD8+ T cells and a subset of NK cells, inflammatory NK cells, showing a statistically significant higher level (**Fig. 2k**). These findings are corroborated in a different cohort of patients, additionally showing a highly significant increase in a tissue-resident signature score for CD8+ T cells (**Fig. 2k**). Thus, together, these observations suggest that SARS-CoV-2 infection of lung cells stimulates CD8+ T cell- and NK cell-attracting cytokines and that these cytotoxic lymphocytes are important for preventing severe symptoms of COVID-19.

Finally, we tested whether the levels of the SARS-CoV-2 host cell protease TMPRSS2 shows similar correlations with the levels of CD8+ T cells and NK cells in the lung. In univariate analyses, baseline TMPRSS2 levels in the lung show significant negative correlations with these lymphocyte levels, although in multivariate analyses, these are only statistically significant for CD8+ T cells and

activated NK cells (**Fig. 3a-c**). The corresponding R and p values are typically also significantly lower than expected by chance (**Fig. 3d,e**). Furthermore, TMPRSS2 mRNA and protein levels strongly correlate ($R=0.8048$, $p<2.2\times 10^{-16}$, **Fig. 3f**) and TMPRSS2 is in the top 2.5 percentile of genes that show the strongest mRNA-protein correlation ($p<2.2\times 10^{-16}$, **Fig. 3g**). Additionally, TMPRSS2 expression tends to correlate negatively with CD8+ T cell- and NK cell-attracting cytokines (**Fig. 3h**). Therefore, albeit typically to a lesser extent, baseline TMPRSS2 expression levels in the lung negatively correlate with the levels of CD8+ T cells and NK cells in a manner similar to ACE2.

Taken together, our observations suggest that a subgroup of individuals may be exceedingly susceptible to developing severe COVID-19 due to concomitant high pre-existing ACE2 and TMPRSS2 expression and low baseline levels of CD8+ T cells and NK cells in the lung (**Fig. 3i**).

Discussion

We investigated the baseline expression levels of the SARS-CoV-2 host cell entry receptor ACE2 and the host cell entry protease TMPRSS2 and the baseline levels of all seven types of anti-viral leukocytes in 1,927 human lung tissue samples. Although SARS-CoV-2 cellular tropism is broad (16-18), we focused on lung tissue. In addition to epithelial cells elsewhere in the respiratory tract, alveolar epithelial cells are thought to be a primary SARS-CoV-2 entry point (16, 28). Consistently, the SARS-CoV-2 receptor ACE2 is expressed in these cells at the mRNA and protein levels (28, 38-40). Moreover, in severely affected COVID-19 patients, the lungs are among the few organs that present with the most life-threatening symptoms. “Cytokine storm”-induced acute respiratory distress syndrome (ARDS), widespread alveolar damage, pneumonia, and progressive respiratory failure have been observed (41, 42). These indications frequently require admission to intensive care units (ICUs) and mechanical ventilation and may ultimately be fatal.

Early after infection, rapid activation of the innate immune system is of paramount importance for the clearance of virus infections. Infected cells typically do so through release of pro-inflammatory cytokines and chemokines, in particular type I and III interferons (19, 20). Notably, however, several

studies have highlighted multiple complexities related specifically to SARS-CoV2 and innate immune system activation at early stages. First, unlike SARS-CoV, SARS-CoV-2-infected lung tissue initially fails to induce a range of immune cell-recruiting molecules, including several interferons (17, 27), suggesting that leukocytes are ineffectively recruited to infected lung shortly after infection. Second, the host cell entry receptor ACE2 has been identified as an interferon target gene (28). Thus, even when interferons are upregulated in order to recruit immune cells, concomitant upregulation of ACE2 expression may in fact exacerbate SARS-CoV-2 infection (28).

These findings suggest that the levels of immune cells that already reside in the lung prior to infection are more critical for dampening SARS-CoV-2 infection at early stages than they are for fighting infections of other viruses. Cytotoxic lymphocytes, including CD8+ T cells and NK cells, are key early responders to virus infections and these are the cells whose baseline levels we here identify as significantly reduced in lung tissue with elevated ACE2 and TMPRSS2 expression. That these immune cells are important in preventing severe COVID-19 is supported by the fact that their levels are significantly higher in bronchoalveolar lavages from mild patients than from severe patients. Therefore, our results suggest that individuals with increased baseline susceptibility to SARS-CoV-2 infection in the lungs may also be less well equipped from the outset to mount a rapid anti-viral cellular immune response (**Fig. 3i**).

Several observations indicate that these cytotoxic lymphocytes are critically important for effective control of SARS-CoV-2 infection. Recent studies showed that CD8+ T cells in peripheral blood are considerably reduced and functionally exhausted in COVID-19 patients, in particular in elderly patients and in severely affected patients that require ICU admission (43-45). Reduced CD8+ T cell counts also predict poor COVID-19 patient survival (43). Additionally, CD8+ T cell- and NK cell-attracting cytokines are upregulated in SARS-CoV-2-infected human lung cells and in lung tissues from COVID-19 patients and the levels of CD8+ T cells and NK cells are higher in bronchoalveolar lavages of mildly affected COVID-19 patients than in severe cases (46, 47).

We found that the five phenotypic parameters, sex, age, BMI, race and smoking history did not statistically significantly contribute to variation in ACE2 expression in human lung tissue, neither in univariate nor in multivariate analyses. This is consistent with some studies but inconsistent with others (42, 48-50). These paradoxical observations may be partially explained by varying gender, age and race distributions within each study cohort.

Further research will be required to elucidate the precise mechanisms of SARS-CoV-2-induced activation of the innate immune system early after infection. However, the link that we identified between high baseline ACE2 and TMPRSS2 expression and reduced cytotoxic lymphocyte levels in human lung tissue prior SARS-CoV-2 infection is striking. It suggests that increased susceptibility to SARS-CoV-2 infection in the lungs may be accompanied by a poorer ability to mount a rapid innate immune response at early stages. This may predict long-term outcome of individuals infected with COVID-19, given that the levels of CD8+ T cell and NK cell are significantly higher in bronchoalveolar lavages of mild cases compared to severe patients (46, 47). Finally, it may contribute to the substantial variation in COVID-19 clinical presentation, ranging from asymptomatic to severe respiratory and other symptoms.

Methods

Discovery dataset and processing

Gene expression data and corresponding phenotype data from human lung tissues (n=578) were obtained from the Genotype-Tissue Expression (GTEx) Portal (<https://gtexportal.org>), managed by the National Institutes of Health (NIH). Gene expression data were publicly available. Access to phenotype data required authorization. The GTEx protocol was previously described (29, 30). Briefly, total RNA was extracted from tissue. Following mRNA isolation, cDNA synthesis and library preparation, samples were subjected to HiSeq2000 or HiSeq2500 Illumina TrueSeq RNA sequencing. Gene expression levels were obtained using RNA-SeQC v1.1.9 (51) and expressed in transcripts per million (TPM). Reported expression levels were log₂-transformed, unless otherwise indicated.

Validation dataset and processing

For validation purposes, the Laval University, University of British-Columbia, Groningen University (LUG) lung tissue dataset (n=1,349) was used. This dataset was accessed via Gene Expression Omnibus (GEO; <https://www.ncbi.nlm.nih.gov/geo>), accession number GSE23546, and was previously described (52). Briefly, total RNA from human lung tissue samples was isolated, quantified, quality-checked and used to generate cDNA, which was amplified and hybridized to Affymetrix gene expression arrays. Arrays were scanned and probe-level gene expression values were normalized using robust multichip average (RMA). These normalized values were obtained from GEO. To collapse probe-level expression data to single expression levels per gene, for each gene the probe with the highest median absolute deviation (MAD) was used. The MAD for each probe p was calculated using equation (1).

$$\text{MAD}(p) = M(|p_i - M(p)|) \quad (1)$$

Herein, M is the median, p_i denotes probe p 's expression level in sample i , and $M(p)$ represents the median signal of probe p .

In silico cytometry

The levels of seven types of leukocytes involved in anti-viral cellular immune response, specifically CD8+ T cells, resting NK cells, activated NK cells, M1 macrophages, CD4+ T cells, dendritic cells and neutrophils, were estimated in the discovery and validation lung tissue samples using a previously described approach (31). Specifically, the following workflow was used. First, only non-log-transformed expression values were used. Thus, where required, expression values for all samples in the discovery and validation datasets were reverse-log₂-transformed using equation 2.

$$c = 2^{c_l} - 1 \quad (2)$$

Herein, c denotes the calculated non-log₂-transformed expression counts and c_l denotes the previously reported log₂-transformed expression counts. Next, to compensate for potential technical differences between signatures and bulk sample gene expression values due to inter-platform variation, bulk-mode batch correction was applied. To ensure robustness, deconvolution was statistically analyzed using 100

permutations. Pearson correlation coefficients R , root mean squared errors (RMSA) and p values are reported on a per-sample level in **Fig. S1a-c** and **Table S1**.

Univariate statistical analyses

Log₂-transformed expression levels of ACE2 in lung tissue samples were compared to the estimated levels of seven leukocyte types or states. Pearson correlation analyses were performed to determine Pearson correlation coefficients R and p values. P values were adjusted at a false discovery rate of 0.05 to yield q values, as previously described (53). Straight lines represent the minimized sum of squares of deviations of the data points with 95% confidence intervals shown. Continuous phenotypic covariates were analyzed in the same way and, additionally, as discrete ordinal categories after binning. Discrete and binned phenotype data were statistically evaluated using Mann-Whitney U tests. All analyses were performed in the R computing environment (R Project for Statistical Computing, Vienna, Austria).

Multivariate regression analyses

Multivariate analyses were performed using standard ordinary least squares regression, summarized in equation 3.

$$Y = \beta_0 + \sum_{k=1}^n (\beta_k X_k) + \varepsilon \quad (3)$$

Herein, β_0 denotes the intercept, while β_k represents the slope of each variable X_k in a model with n variables and ε denotes the random error component. These analyses was performed using R .

Messenger RNA and protein levels in human cells

Available ACE2 and TMPRSS2 mRNA and corresponding protein levels in 52 and 124 human cell lines, respectively, were obtained from references (54, 55). The correlations between mRNA and protein levels were analyzed by linear regression analysis using Pearson correlations. Pearson coefficients R for mRNA-protein level correlations were also determined for 12,015 other genes. To test whether the ACE2 and TMPRSS2 coefficients and p values were statistically significantly lower than for other genes, one-sample t tests were used.

Messenger RNA and protein levels in human tissues

Two types of analyses were performed to compare mRNA and protein levels in human tissues. First, mRNA expression levels from 40 human tissues were obtained from the Human Protein Atlas (<https://www.proteinatlas.org>). These represented the consensus normalized mRNA expression levels from three sources, specifically, Human Protein Atlas in-house RNAseq data, RNAseq data from the Genotype-Tissue Expression (GTEx) project and CAGE data from FANTOM5 project. Corresponding ordinal human tissue protein expression levels ('not detected', 'low', 'high') were also obtained from the Human Protein Atlas. These were based on immunohistochemical staining of the tissues using DAB (3,3'-diaminobenzidine)-labeled antibodies (HPA000288, CAB026174), followed by knowledge-based annotation, as described on said website. A Kruskal-Wallis test was performed to assess whether mRNA and protein levels significantly correlated. Second, a meta-analysis was performed. For this, mRNA and protein expression levels were obtained from nine different sources. Tissue mRNA levels were obtained from six sources, as determined by Northern blot (56), quantitative RT-PCR (57), microarray hybridization (58), RNA sequencing (59) and cap analysis of gene expression (60). Tissue protein levels were obtained from three sources, as determined by mass spectrometry (61) and immunohistochemistry (39, 62). For each source and tissue, mRNA and protein expression levels were scored as 'not detected', 'low', 'intermediate' or 'high' and these received scores of 0-3, respectively. For each tissue, final mRNA and protein scores were calculated by averaging and scores from the respective six and three sources (**Table S4**). Strength and significance level of the correlation between the final scores were determined by linear regression analysis using Pearson correlation.

Cytokine levels in SARS-CoV-2-infected lung cells

SARS-CoV-2-induced fold increases in the expression levels of eight cytotoxic lymphocyte-attracting cytokines, CCL2-5, CXCL9, CXCL10, CXCL16 and IL18, were determined from reference (27). These represent fold increase in expression in Calu-3 lung cells, 24 hours after infection with SARS-CoV-2 at a multiplicity of infection of 2, compared to uninfected Calu-3 cells.

Cytokine levels in control and COVID-19 lung tissues

Baseline levels of above eight cytokines in lung tissues were obtained from the GTEx project, as described above, and compared to the baseline levels of ACE2, TMPRSS2, CD8+ T cells, resting and activated NK cells in these tissues, estimated as described above. Their levels were compared using Spearman's rank correlations (R and p values). For comparison of cytokine levels in post-mortem COVID-19 lung tissues ($n=2$) to those in healthy, uninfected lung tissues ($n=2$), fold increases were determined following RNAseq analyses and previously reported (27).

Lymphocyte levels in COVID-19 bronchoalveolar lavages

The levels of CD8+ T cells, NK cells and inflammatory NK cells in bronchoalveolar lavages from mild ($n=2$) and severe ($n=22$) COVID-19 patients were reported elsewhere and determined using single-cell RNAseq (46). Statistical significance levels were assessed using Mann-Whitney U tests. The levels of T cells and NK cells, as well as CD8+ T cell tissue-resident signature score, in bronchoalveolar lavages from moderate ($n=3$) and severe/critical ($n=5$) COVID-19 patients were reported in another study (47).

Acknowledgements

I thank Dr. Marianna Datseris, M.D. for critically reading the manuscript. This work was supported by the School of Biomedical Sciences, Queensland University of Technology. This study used publicly available and controlled data from the Genotype-Tissue Expression (GTEx) Project. GTEx was supported by the Common Fund of the Office of the Director of the National Institutes of Health (commonfund.nih.gov/GTEx). Additional funds were provided by the NCI, NHGRI, NHLBI, NIDA, NIMH, and NINDS. Donors were enrolled at Biospecimen Source Sites funded by NCI\Leidos Biomedical Research, Inc. subcontracts to the National Disease Research Interchange (10XS170), Roswell Park Cancer Institute (10XS171), and Science Care, Inc. (X10S172). The Laboratory, Data Analysis, and Coordinating Center (LDACC) was funded through a contract (HHSN268201000029C) to the The Broad Institute, Inc. Biorepository operations were funded through a Leidos Biomedical Research, Inc. subcontract to Van Andel Research Institute (10ST1035). Additional data repository and project management were provided by Leidos Biomedical Research, Inc. (HHSN261200800001E). The

Brain Bank was supported supplements to University of Miami grant DA006227. Statistical Methods development grants were made to the University of Geneva (MH090941 & MH101814), the University of Chicago (MH090951, MH090937, MH101825, & MH101820), the University of North Carolina - Chapel Hill (MH090936), North Carolina State University (MH101819), Harvard University (MH090948), Stanford University (MH101782), Washington University (MH101810), and to the University of Pennsylvania (MH101822). The datasets used for the analyses described in this study were obtained from dbGaP at <http://www.ncbi.nlm.nih.gov/gap> through dbGaP accession number phs000424.v8.p2.

References

1. Coronaviridae Study Group of the International Committee on Taxonomy of V. 2020. The species Severe acute respiratory syndrome-related coronavirus: classifying 2019-nCoV and naming it SARS-CoV-2. *Nat Microbiol* 5:536-544. <https://doi.org/10.1038/s41564-020-0695-z>.
2. Liu Y, Yan LM, Wan L, Xiang TX, Le A, Liu JM, Peiris M, Poon LLM, Zhang W. 2020. Viral dynamics in mild and severe cases of COVID-19. *Lancet Infect Dis* [https://doi.org/10.1016/S1473-3099\(20\)30232-2](https://doi.org/10.1016/S1473-3099(20)30232-2).
3. Gattinoni L, Chiumello D, Caironi P, Busana M, Romitti F, Brazzi L, Camporota L. 2020. COVID-19 pneumonia: different respiratory treatments for different phenotypes? *Intensive Care Med* <https://doi.org/10.1007/s00134-020-06033-2>.
4. Xie M and Chen Q. 2020. Insight into 2019 novel coronavirus - An updated interim review and lessons from SARS-CoV and MERS-CoV. *Int J Infect Dis* 94:119-124. <https://doi.org/10.1016/j.ijid.2020.03.071>.
5. 2020. Coronavirus disease 2019 (COVID-19), Situation Report 102. World Health Organization
6. Li R, Pei S, Chen B, Song Y, Zhang T, Yang W, Shaman J. 2020. Substantial undocumented infection facilitates the rapid dissemination of novel coronavirus (SARS-CoV-2). *Science* 368:489-493. <https://doi.org/10.1126/science.abb3221>.
7. Hoffmann M, Kleine-Weber H, Schroeder S, Kruger N, Herrler T, Erichsen S, Schiergens TS, Herrler G, Wu NH, Nitsche A, Muller MA, Drosten C, Pohlmann S. 2020. SARS-CoV-2 Cell Entry Depends on ACE2 and TMPRSS2 and Is Blocked by a Clinically Proven Protease Inhibitor. *Cell* 181:271-280 e8. <https://doi.org/10.1016/j.cell.2020.02.052>.
8. Zhou P, Yang XL, Wang XG, Hu B, Zhang L, Zhang W, Si HR, Zhu Y, Li B, Huang CL, Chen HD, Chen J, Luo Y, Guo H, Jiang RD, Liu MQ, Chen Y, Shen XR, Wang X, Zheng XS, Zhao K, Chen QJ, Deng F, Liu LL, Yan B, Zhan FX, Wang YY, Xiao GF, Shi ZL. 2020. A pneumonia outbreak associated with a new coronavirus of probable bat origin. *Nature* 579:270-273. <https://doi.org/10.1038/s41586-020-2012-7>.
9. Wrapp D, Wang N, Corbett KS, Goldsmith JA, Hsieh CL, Abiona O, Graham BS, McLellan JS. 2020. Cryo-EM structure of the 2019-nCoV spike in the prefusion conformation. *Science* 367:1260-1263. <https://doi.org/10.1126/science.abb2507>.
10. Hofmann H, Geier M, Marzi A, Krumbiegel M, Peipp M, Fey GH, Gramberg T, Pohlmann S. 2004. Susceptibility to SARS coronavirus S protein-driven infection correlates with expression of

- angiotensin converting enzyme 2 and infection can be blocked by soluble receptor. *Biochem Biophys Res Commun* 319:1216-21. <https://doi.org/10.1016/j.bbrc.2004.05.114>.
11. Mossel EC, Huang C, Narayanan K, Makino S, Tesh RB, Peters CJ. 2005. Exogenous ACE2 expression allows refractory cell lines to support severe acute respiratory syndrome coronavirus replication. *J Virol* 79:3846-50. <https://doi.org/10.1128/JVI.79.6.3846-3850.2005>.
 12. Li W, Moore MJ, Vasilieva N, Sui J, Wong SK, Berne MA, Somasundaran M, Sullivan JL, Luzuriaga K, Greenough TC, Choe H, Farzan M. 2003. Angiotensin-converting enzyme 2 is a functional receptor for the SARS coronavirus. *Nature* 426:450-4. <https://doi.org/10.1038/nature02145>.
 13. Fang L, Karakiulakis G, Roth M. 2020. Are patients with hypertension and diabetes mellitus at increased risk for COVID-19 infection? *Lancet Respir Med* 8:e21. [https://doi.org/10.1016/S2213-2600\(20\)30116-8](https://doi.org/10.1016/S2213-2600(20)30116-8).
 14. Guo J, Huang Z, Lin L, Lv J. 2020. Coronavirus Disease 2019 (COVID-19) and Cardiovascular Disease: A Viewpoint on the Potential Influence of Angiotensin-Converting Enzyme Inhibitors/Angiotensin Receptor Blockers on Onset and Severity of Severe Acute Respiratory Syndrome Coronavirus 2 Infection. *J Am Heart Assoc* 9:e016219. <https://doi.org/10.1161/JAHA.120.016219>.
 15. Zhuang MW, Cheng Y, Zhang J, Jiang XM, Wang L, Deng J, Wang PH. 2020. Increasing host cellular receptor-angiotensin-converting enzyme 2 expression by coronavirus may facilitate 2019-nCoV (or SARS-CoV-2) infection. *J Med Virol* <https://doi.org/10.1002/jmv.26139>.
 16. Sungnak W, Huang N, Becavin C, Berg M, Queen R, Litvinukova M, Talavera-Lopez C, Maatz H, Reichart D, Sampaziotis F, Worlock KB, Yoshida M, Barnes JL, Network HCALB. 2020. SARS-CoV-2 entry factors are highly expressed in nasal epithelial cells together with innate immune genes. *Nat Med* <https://doi.org/10.1038/s41591-020-0868-6>.
 17. Chu H, Chan JF, Wang Y, Yuen TT, Chai Y, Hou Y, Shuai H, Yang D, Hu B, Huang X, Zhang X, Cai JP, Zhou J, Yuan S, Kok KH, To KK, Chan IH, Zhang AJ, Sit KY, Au WK, Yuen KY. 2020. Comparative replication and immune activation profiles of SARS-CoV-2 and SARS-CoV in human lungs: an ex vivo study with implications for the pathogenesis of COVID-19. *Clin Infect Dis* <https://doi.org/10.1093/cid/ciaa410>.
 18. Chu H, Chan JFW, Yuen TTT, Shuai H, Yuan S, Wang Y, Hu B, Yip CCY, Tsang JOL, Huang X, Chai Y, Yang D, Hou Y, Chik KKH, Zhang X, Fung AYW, Tsoi HY, Cai JP, Chan WM, Ip JD, Chu AWH, Zhou J, Lung DC, Kok KH, To KKW, Tsang OTY, Chan KH, Yuen KY. 2020. Comparative tropism, replication kinetics, and cell damage profiling of SARS-CoV-2 and SARS-CoV with implications for clinical manifestations, transmissibility, and laboratory studies of COVID-19: an observational study. *Lancet Microbe* April 21, 2020:1-10. [https://doi.org/10.1016/S2666-5247\(20\)30004-5](https://doi.org/10.1016/S2666-5247(20)30004-5).
 19. Newton AH, Cardani A, Braciale TJ. 2016. The host immune response in respiratory virus infection: balancing virus clearance and immunopathology. *Semin Immunopathol* 38:471-82. <https://doi.org/10.1007/s00281-016-0558-0>.
 20. Crouse J, Kalinke U, Oxenius A. 2015. Regulation of antiviral T cell responses by type I interferons. *Nat Rev Immunol* 15:231-42. <https://doi.org/10.1038/nri3806>.
 21. Schmidt ME and Varga SM. 2018. The CD8 T Cell Response to Respiratory Virus Infections. *Front Immunol* 9:678. <https://doi.org/10.3389/fimmu.2018.00678>.
 22. Hammer Q, Ruckert T, Romagnani C. 2018. Natural killer cell specificity for viral infections. *Nat Immunol* 19:800-808. <https://doi.org/10.1038/s41590-018-0163-6>.
 23. Cook PC and MacDonald AS. 2016. Dendritic cells in lung immunopathology. *Semin Immunopathol* 38:449-60. <https://doi.org/10.1007/s00281-016-0571-3>.
 24. Sant AJ and McMichael A. 2012. Revealing the role of CD4(+) T cells in viral immunity. *J Exp Med* 209:1391-5. <https://doi.org/10.1084/jem.20121517>.
 25. Harper RW. 2017. Partners in Crime: Epithelial Priming of Macrophages during Viral Infection. *Am J Respir Cell Mol Biol* 57:145-146. <https://doi.org/10.1165/rcmb.2017-0153ED>.

26. Galani IE and Andreakos E. 2015. Neutrophils in viral infections: Current concepts and caveats. *J Leukoc Biol* 98:557-64. <https://doi.org/10.1189/jlb.4VMR1114-555R>.
27. Blanco-Melo D, Nilsson-Payant BE, Liu WC, Uhl S, Hoagland D, Moller R, Jordan TX, Oishi K, Panis M, Sachs D, Wang TT, Schwartz RE, Lim JK, Albrecht RA, tenOever BR. 2020. Imbalanced Host Response to SARS-CoV-2 Drives Development of COVID-19. *Cell* 181:1036-1045 e9. <https://doi.org/10.1016/j.cell.2020.04.026>.
28. Ziegler CGK, Allon SJ, Nyquist SK, Mbano IM, Miao VN, Tzouanas CN, Cao Y, Yousif AS, Bals J, Hauser BM, Feldman J, Muus C, Wadsworth MH, 2nd, Kazer SW, Hughes TK, Doran B, Gatter GJ, Vukovic M, Taliaferro F, Mead BE, Guo Z, Wang JP, Gras D, Plaisant M, Ansari M, Angelidis I, Adler H, Sucre JMS, Taylor CJ, Lin B, Waghray A, Mitsialis V, Dwyer DF, Buchheit KM, Boyce JA, Barrett NA, Laidlaw TM, Carroll SL, Colonna L, Tkachev V, Peterson CW, Yu A, Zheng HB, Gideon HP, Winchell CG, Lin PL, Bingle CD, Snapper SB, Kropski JA, et al. 2020. SARS-CoV-2 Receptor ACE2 Is an Interferon-Stimulated Gene in Human Airway Epithelial Cells and Is Detected in Specific Cell Subsets across Tissues. *Cell* 181:1016-1035 e19. <https://doi.org/10.1016/j.cell.2020.04.035>.
29. Consortium GT. 2013. The Genotype-Tissue Expression (GTEx) project. *Nat Genet* 45:580-5. <https://doi.org/10.1038/ng.2653>.
30. Consortium GT, Laboratory DA, Coordinating Center -Analysis Working G, Statistical Methods groups-Analysis Working G, Enhancing Gg, Fund NIHC, Nih/Nci, Nih/Nhgri, Nih/Nimh, Nih/Nida, Biospecimen Collection Source Site N, Biospecimen Collection Source Site R, Biospecimen Core Resource V, Brain Bank Repository-University of Miami Brain Endowment B, Leidos Biomedical-Project M, Study E, Genome Browser Data I, Visualization EBI, Genome Browser Data I, Visualization-Ucsc Genomics Institute UoCSC, Lead a, Laboratory DA, Coordinating C, management NIHp, Biospecimen c, Pathology, e QTLmwg, Battle A, Brown CD, Engelhardt BE, Montgomery SB. 2017. Genetic effects on gene expression across human tissues. *Nature* 550:204-213. <https://doi.org/10.1038/nature24277>.
31. Newman AM, Liu CL, Green MR, Gentles AJ, Feng W, Xu Y, Hoang CD, Diehn M, Alizadeh AA. 2015. Robust enumeration of cell subsets from tissue expression profiles. *Nat Methods* 12:453-7. <https://doi.org/10.1038/nmeth.3337>.
32. Brown CE, Vishwanath RP, Aguilar B, Starr R, Najbauer J, Aboody KS, Jensen MC. 2007. Tumor-derived chemokine MCP-1/CCL2 is sufficient for mediating tumor tropism of adoptively transferred T cells. *J Immunol* 179:3332-41. <https://doi.org/10.4049/jimmunol.179.5.3332>.
33. Serody JS, Burkett SE, Panoskaltsis-Mortari A, Ng-Cashin J, McMahon E, Matsushima GK, Lira SA, Cook DN, Blazar BR. 2000. T-lymphocyte production of macrophage inflammatory protein-1alpha is critical to the recruitment of CD8(+) T cells to the liver, lung, and spleen during graft-versus-host disease. *Blood* 96:2973-80.
34. Zumwalt TJ, Arnold M, Goel A, Boland CR. 2015. Active secretion of CXCL10 and CCL5 from colorectal cancer microenvironments associates with GranzymeB+ CD8+ T-cell infiltration. *Oncotarget* 6:2981-91. <https://doi.org/10.18632/oncotarget.3205>.
35. Spranger S, Dai D, Horton B, Gajewski TF. 2017. Tumor-Residing Batf3 Dendritic Cells Are Required for Effector T Cell Trafficking and Adoptive T Cell Therapy. *Cancer Cell* 31:711-723 e4. <https://doi.org/10.1016/j.ccell.2017.04.003>.
36. Wendel M, Galani IE, Suri-Payer E, Cerwenka A. 2008. Natural killer cell accumulation in tumors is dependent on IFN-gamma and CXCR3 ligands. *Cancer Res* 68:8437-45. <https://doi.org/10.1158/0008-5472.CAN-08-1440>.
37. Fan Z, Yu P, Wang Y, Wang Y, Fu ML, Liu W, Sun Y, Fu YX. 2006. NK-cell activation by LIGHT triggers tumor-specific CD8+ T-cell immunity to reject established tumors. *Blood* 107:1342-51. <https://doi.org/10.1182/blood-2005-08-3485>.
38. Bertram S, Heurich A, Lavender H, Gierer S, Danisch S, Perin P, Lucas JM, Nelson PS, Pohlmann S, Soilleux EJ. 2012. Influenza and SARS-coronavirus activating proteases TMPRSS2 and HAT are

- expressed at multiple sites in human respiratory and gastrointestinal tracts. *PLoS One* 7:e35876. <https://doi.org/10.1371/journal.pone.0035876>.
39. Hamming I, Timens W, Bulthuis ML, Lely AT, Navis G, van Goor H. 2004. Tissue distribution of ACE2 protein, the functional receptor for SARS coronavirus. A first step in understanding SARS pathogenesis. *J Pathol* 203:631-7. <https://doi.org/10.1002/path.1570>.
 40. Zou X, Chen K, Zou J, Han P, Hao J, Han Z. 2020. Single-cell RNA-seq data analysis on the receptor ACE2 expression reveals the potential risk of different human organs vulnerable to 2019-nCoV infection. *Front Med* <https://doi.org/10.1007/s11684-020-0754-0>.
 41. Huang C, Wang Y, Li X, Ren L, Zhao J, Hu Y, Zhang L, Fan G, Xu J, Gu X, Cheng Z, Yu T, Xia J, Wei Y, Wu W, Xie X, Yin W, Li H, Liu M, Xiao Y, Gao H, Guo L, Xie J, Wang G, Jiang R, Gao Z, Jin Q, Wang J, Cao B. 2020. Clinical features of patients infected with 2019 novel coronavirus in Wuhan, China. *Lancet* 395:497-506. [https://doi.org/10.1016/S0140-6736\(20\)30183-5](https://doi.org/10.1016/S0140-6736(20)30183-5).
 42. Chan JF, Yuan S, Kok KH, To KK, Chu H, Yang J, Xing F, Liu J, Yip CC, Poon RW, Tsoi HW, Lo SK, Chan KH, Poon VK, Chan WM, Ip JD, Cai JP, Cheng VC, Chen H, Hui CK, Yuen KY. 2020. A familial cluster of pneumonia associated with the 2019 novel coronavirus indicating person-to-person transmission: a study of a family cluster. *Lancet* 395:514-523. [https://doi.org/10.1016/S0140-6736\(20\)30154-9](https://doi.org/10.1016/S0140-6736(20)30154-9).
 43. Diao B, Wang C, Tan Y, Chen X, Liu Y, Ning L, Chen L, Li M, Liu Y, Wang G, Yuan Z, Feng Z, Zhang Y, Wu Y, Chen Y. 2020. Reduction and Functional Exhaustion of T Cells in Patients With Coronavirus Disease 2019 (COVID-19). *Front Immunol* 11:827. <https://doi.org/10.3389/fimmu.2020.00827>.
 44. Zheng M, Gao Y, Wang G, Song G, Liu S, Sun D, Xu Y, Tian Z. 2020. Functional exhaustion of antiviral lymphocytes in COVID-19 patients. *Cell Mol Immunol* <https://doi.org/10.1038/s41423-020-0402-2>.
 45. Liu J, Li S, Liu J, Liang B, Wang X, Wang H, Li W, Tong Q, Yi J, Zhao L, Xiong L, Guo C, Tian J, Luo J, Yao J, Pang R, Shen H, Peng C, Liu T, Zhang Q, Wu J, Xu L, Lu S, Wang B, Weng Z, Han C, Zhu H, Zhou R, Zhou H, Chen X, Ye P, Zhu B, Wang L, Zhou W, He S, He Y, Jie S, Wei P, Zhang J, Lu Y, Wang W, Zhang L, Li L, Zhou F, Wang J, Dittmer U, Lu M, Hu Y, Yang D, et al. 2020. Longitudinal characteristics of lymphocyte responses and cytokine profiles in the peripheral blood of SARS-CoV-2 infected patients. *EBioMedicine* 55:102763. <https://doi.org/10.1016/j.ebiom.2020.102763>.
 46. Wauters E, Van Mol P, Garg AD, Jansen S, Van Herck Y, Vanderbeke L, Bassez A, Boeckx B, Malengier-Devlies B, Timmerman A, Van Brussel T, Van Buyten T, Schepers R, Heylen E, Dauwe D, Doooms C, Gunst J, Hermans G, Meersseman P, Testelmans D, Yserbyt J, Matthys P, Tejpar S, CONTAGIOUS collaborators, Neyts J, Wauters J, Qian J, Lambrechts D. 2020. Discriminating mild from critical COVID-19 by innate and adaptive immune single-cell profiling of bronchoalveolar lavages. *bioRxiv Preprint:10 July 2020*. <https://doi.org/10.1101/2020.07.09.196519>.
 47. Liao M, Liu Y, Yuan J, Wen Y, Xu G, Zhao J, Cheng L, Li J, Wang X, Wang F, Liu L, Amit I, Zhang S, Zhang Z. 2020. Single-cell landscape of bronchoalveolar immune cells in patients with COVID-19. *Nat Med* 26:842-844. <https://doi.org/10.1038/s41591-020-0901-9>.
 48. Lloyd-Sherlock P, Ebrahim S, Geffen L, McKee M. 2020. Bearing the brunt of covid-19: older people in low and middle income countries. *BMJ* 368:m1052. <https://doi.org/10.1136/bmj.m1052>.
 49. Yang X, Yu Y, Xu J, Shu H, Xia J, Liu H, Wu Y, Zhang L, Yu Z, Fang M, Yu T, Wang Y, Pan S, Zou X, Yuan S, Shang Y. 2020. Clinical course and outcomes of critically ill patients with SARS-CoV-2 pneumonia in Wuhan, China: a single-centered, retrospective, observational study. *Lancet Respir Med* [https://doi.org/10.1016/S2213-2600\(20\)30079-5](https://doi.org/10.1016/S2213-2600(20)30079-5).
 50. Smith JC, Sausville EL, Girish V, Yuan ML, Vasudevan A, John KM, Sheltzer JM. 2020. Cigarette Smoke Exposure and Inflammatory Signaling Increase the Expression of the SARS-CoV-2 Receptor ACE2 in the Respiratory Tract. *Dev Cell* 53:514-529 e3. <https://doi.org/10.1016/j.devcel.2020.05.012>.

51. DeLuca DS, Levin JZ, Sivachenko A, Fennell T, Nazaire MD, Williams C, Reich M, Winckler W, Getz G. 2012. RNA-SeQC: RNA-seq metrics for quality control and process optimization. *Bioinformatics* 28:1530-2. <https://doi.org/10.1093/bioinformatics/bts196>.
52. Obeidat M, Hao K, Bosse Y, Nickle DC, Nie Y, Postma DS, Laviolette M, Sandford AJ, Daley DD, Hogg JC, Elliott WM, Fishbane N, Timens W, Hysi PG, Kaprio J, Wilson JF, Hui J, Rawal R, Schulz H, Stubbe B, Hayward C, Polasek O, Jarvelin MR, Zhao JH, Jarvis D, Kahonen M, Franceschini N, North KE, Loth DW, Brusselle GG, Smith AV, Gudnason V, Bartz TM, Wilk JB, O'Connor GT, Cassano PA, Tang W, Wain LV, Soler Artigas M, Gharib SA, Strachan DP, Sin DD, Tobin MD, London SJ, Hall IP, Pare PD. 2015. Molecular mechanisms underlying variations in lung function: a systems genetics analysis. *Lancet Respir Med* 3:782-95. [https://doi.org/10.1016/S2213-2600\(15\)00380-X](https://doi.org/10.1016/S2213-2600(15)00380-X).
53. Benjamini Y and Hochberg Y. 1995. Controlling the False Discovery Rate: A practical and powerful approach to multiple testing. *J R Stat Soc Ser B-Stat Methodol* 57:289-300.
54. Ghandi M, Huang FW, Jane-Valbuena J, Kryukov GV, Lo CC, McDonald ER, 3rd, Barretina J, Gelfand ET, Bielski CM, Li H, Hu K, Andreev-Drakhlin AY, Kim J, Hess JM, Haas BJ, Aguet F, Weir BA, Rothberg MV, Paoletta BR, Lawrence MS, Akbani R, Lu Y, Tiv HL, Gokhale PC, de Weck A, Mansour AA, Oh C, Shih J, Hadi K, Rosen Y, Bistline J, Venkatesan K, Reddy A, Sonkin D, Liu M, Lehar J, Korn JM, Porter DA, Jones MD, Golji J, Caponigro G, Taylor JE, Dunning CM, Creech AL, Warren AC, McFarland JM, Zamanighomi M, Kauffmann A, Stransky N, et al. 2019. Next-generation characterization of the Cancer Cell Line Encyclopedia. *Nature* 569:503-508. <https://doi.org/10.1038/s41586-019-1186-3>.
55. Nusinow DP, Szpyt J, Ghandi M, Rose CM, McDonald ER, 3rd, Kalocsay M, Jane-Valbuena J, Gelfand E, Schweppe DK, Jedrychowski M, Golji J, Porter DA, Rejtar T, Wang YK, Kryukov GV, Stegmeier F, Erickson BK, Garraway LA, Sellers WR, Gygi SP. 2020. Quantitative Proteomics of the Cancer Cell Line Encyclopedia. *Cell* 180:387-402 e16. <https://doi.org/10.1016/j.cell.2019.12.023>.
56. Tipnis SR, Hooper NM, Hyde R, Karran E, Christie G, Turner AJ. 2000. A human homolog of angiotensin-converting enzyme. Cloning and functional expression as a captopril-insensitive carboxypeptidase. *J Biol Chem* 275:33238-43. <https://doi.org/10.1074/jbc.M002615200>.
57. Harmer D, Gilbert M, Borman R, Clark KL. 2002. Quantitative mRNA expression profiling of ACE 2, a novel homologue of angiotensin converting enzyme. *FEBS Lett* 532:107-10. [https://doi.org/10.1016/s0014-5793\(02\)03640-2](https://doi.org/10.1016/s0014-5793(02)03640-2).
58. Wu C, Jin X, Tsueng G, Afrasiabi C, Su AI. 2016. BioGPS: building your own mash-up of gene annotations and expression profiles. *Nucleic Acids Res* 44:D313-6. <https://doi.org/10.1093/nar/gkv1104>.
59. Uhlen M, Zhang C, Lee S, Sjostedt E, Fagerberg L, Bidkhorji G, Benfeitas R, Arif M, Liu Z, Edfors F, Sanli K, von Feilitzen K, Oksvold P, Lundberg E, Hober S, Nilsson P, Mattsson J, Schwenk JM, Brunnstrom H, Glimelius B, Sjoblom T, Edqvist PH, Djureinovic D, Micke P, Lindskog C, Mardinoglu A, Ponten F. 2017. A pathology atlas of the human cancer transcriptome. *Science* 357:<https://doi.org/10.1126/science.aan2507>.
60. Consortium F, the RP, Clst, Forrest AR, Kawaji H, Rehli M, Baillie JK, de Hoon MJ, Haberle V, Lassmann T, Kulakovskiy IV, Lizio M, Itoh M, Andersson R, Mungall CJ, Meehan TF, Schmeier S, Bertin N, Jorgensen M, Dimont E, Arner E, Schmidl C, Schaefer U, Medvedeva YA, Plessy C, Vitezic M, Severin J, Semple C, Ishizu Y, Young RS, Francescato M, Alam I, Albanese D, Altschuler GM, Arakawa T, Archer JA, Arner P, Babina M, Rennie S, Balwierz PJ, Beckhouse AG, Pradhan-Bhatt S, Blake JA, Blumenthal A, Bodega B, Bonetti A, Briggs J, Brombacher F, Burroughs AM, et al. 2014. A promoter-level mammalian expression atlas. *Nature* 507:462-70. <https://doi.org/10.1038/nature13182>.
61. Kim MS, Pinto SM, Getnet D, Nirujogi RS, Manda SS, Chaerkady R, Madugundu AK, Kelkar DS, Isserlin R, Jain S, Thomas JK, Muthusamy B, Leal-Rojas P, Kumar P, Sahasrabudde NA, Balakrishnan L, Advani J, George B, Renuse S, Selvan LD, Patil AH, Nanjappa V, Radhakrishnan A, Prasad S, Subbannayya T, Raju R, Kumar M, Sreenivasamurthy SK, Marimuthu A, Sathe GJ,

- Chavan S, Datta KK, Subbannayya Y, Sahu A, Yelamanchi SD, Jayaram S, Rajagopalan P, Sharma J, Murthy KR, Syed N, Goel R, Khan AA, Ahmad S, Dey G, Mudgal K, Chatterjee A, Huang TC, Zhong J, Wu X, et al. 2014. A draft map of the human proteome. *Nature* 509:575-81. <https://doi.org/10.1038/nature13302>.
62. Thul PJ, Akesson L, Wiking M, Mahdessian D, Geladaki A, Ait Blal H, Alm T, Asplund A, Bjork L, Breckels LM, Backstrom A, Danielsson F, Fagerberg L, Fall J, Gatto L, Gnann C, Hober S, Hjelmare M, Johansson F, Lee S, Lindskog C, Mulder J, Mulvey CM, Nilsson P, Oksvold P, Rockberg J, Schutten R, Schwenk JM, Sivertsson A, Sjostedt E, Skogs M, Stadler C, Sullivan DP, Tegel H, Winsnes C, Zhang C, Zwahlen M, Mardinoglu A, Ponten F, von Feilitzen K, Lilley KS, Uhlen M, Lundberg E. 2017. A subcellular map of the human proteome. *Science* 356:<https://doi.org/10.1126/science.aal3321>.

Figure 1

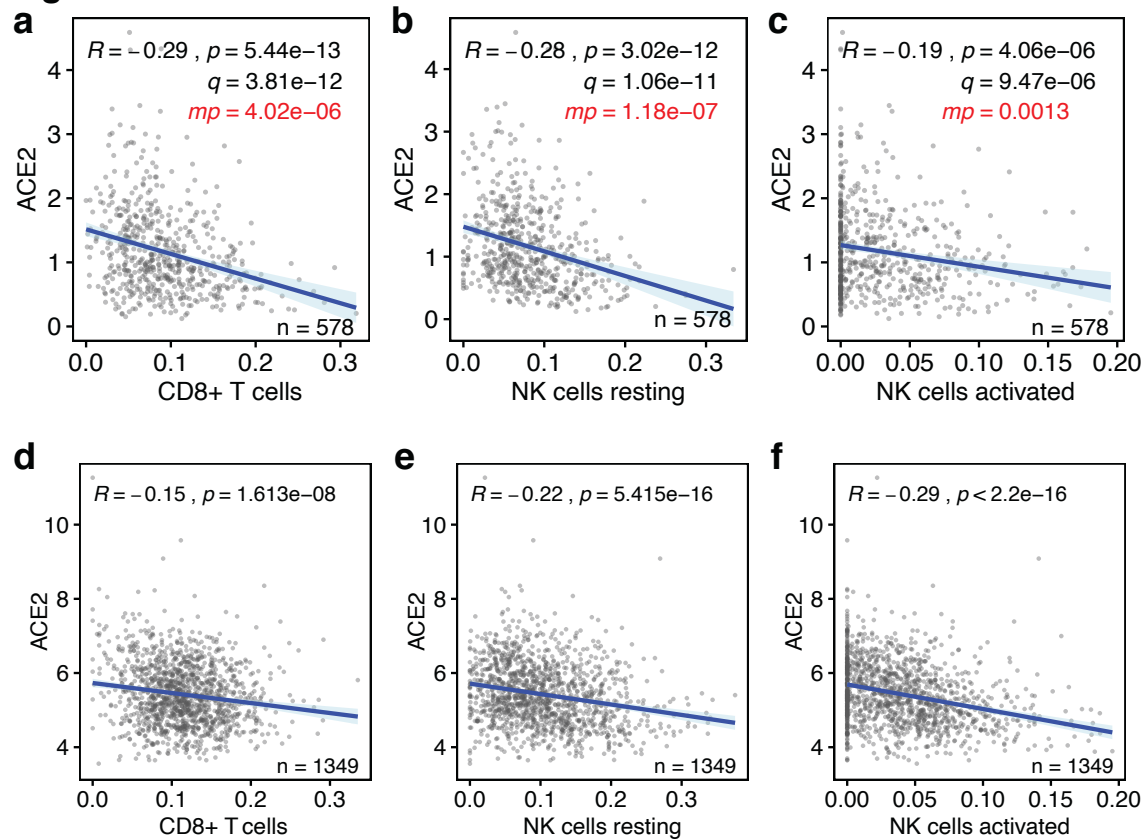


Figure 1. Baseline levels of cytotoxic lymphocytes inversely correlate with ACE2 expression in the lung.

(a-c) The correlations between the baseline levels of CD8+ T cells, resting NK cells and activated NK cells (x-axes) and the those of the SARS-CoV-2 host cell receptor ACE2 (y-axes) in human lung tissue are shown. Data are from the GTEx dataset (n=578). **(d-f)** The same correlations are shown for lung tissues in the LUG dataset (n=1,349). Regression lines and 95% confidence intervals are shown. R and p values: Pearson correlations; q values: Benjamini-Hochberg-adjusted p values using a false discovery rate of 0.05; mp values: multivariate p values (see Table S3).

Figure 2

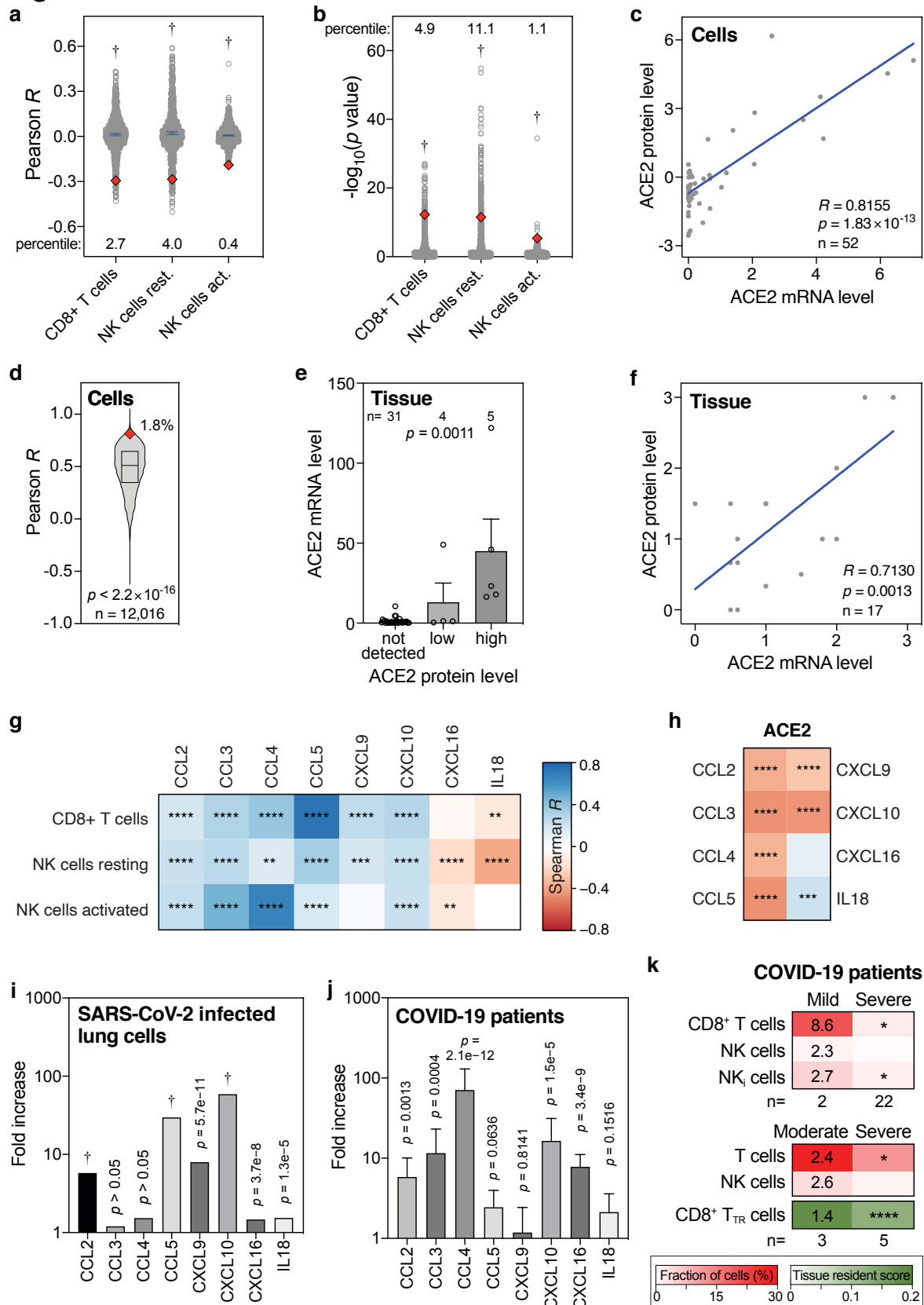


Figure 2. Levels of ACE2 mRNA, ACE2 protein, CD8+ T cells, NK cells and cytokines in lung cells, lung tissues and COVID-19 patient samples.

(a, b) Pearson R and $-\log_{10}(p)$ values) of correlations between 1000 randomly sampled genes and the levels of indicated lymphocytes in lung tissues were determined and plotted. ACE2 Pearson R and p values are shown as red diamonds. Blue lines indicate means with 95% confidence intervals. Percentiles for ACE2 with respect to the 1000 random R and p values are shown. Data are from the GTEx dataset ($n=578$). P values: one-sample t tests. **(c)** Correlations between ACE2 mRNA and protein levels in 52 cell lines. R and p values: Pearson correlations. **(d)** Pearson correlation R values between mRNA and protein levels of 12,016 genes are compared to the ACE2 R coefficient (red diamond). The box represents the median and interquartile range. The ACE2 R percentile is also shown. P value: one-sample t test. **(e)** Bar graph showing the correlation between ACE2 mRNA and protein levels in human tissues. Means with standard errors of the means are shown. Samples are from the Human Protein Atlas. P value: Kruskal-Wallis test. **(f)** Meta-analysis scatter plot showing the correlation between ACE2 mRNA and protein levels in 17 human tissues. Data are from 9 different studies, as detailed in Table S4. P value: Pearson correlation. **(g, h)** Heatmaps showing Spearman correlations between the levels of ACE2 or indicated cytotoxic lymphocytes and eight cytokines that recruit these cells in human lung tissues from the GTEx dataset ($n=578$). Colors of tiles represent Spearman R , as per scale bar on the right. Spearman significance levels are shown by asterisks. See also Fig. S5. **(i, j)** Fold increase in expression levels of indicated cytokines in Calu-3 lung cells 24 hours after SARS-CoV-2 infection compared to uninfected Calu-3 cells (i), and in post-mortem COVID-19 lung tissues ($n=2$) to those in healthy, uninfected lung tissues ($n=2$) (j). **(k)** Comparison of indicated fractions of lymphocyte levels in bronchoalveolar lavages of mild/moderate and severe COVID-19 patients, as determined in two separate studies (46, 47). The second also determined a tissue resident (TR) score for CD8+ T cells. Numbers in the mild/moderate column on the left show fold increase compared to the respective severe cases on the right. Asterisks in the severe column on the right represent statistical significance levels, as determined by Mann-Whitney U tests (top panel), or t tests (middle and bottom panels) comparing mild/moderate to severe cases. P value abbreviations: *, $p<0.05$; **, $p<0.01$; ***, $p<0.001$; ****, $p<0.0001$; †, $p<2.2\times 10^{-16}$.

Figure 3

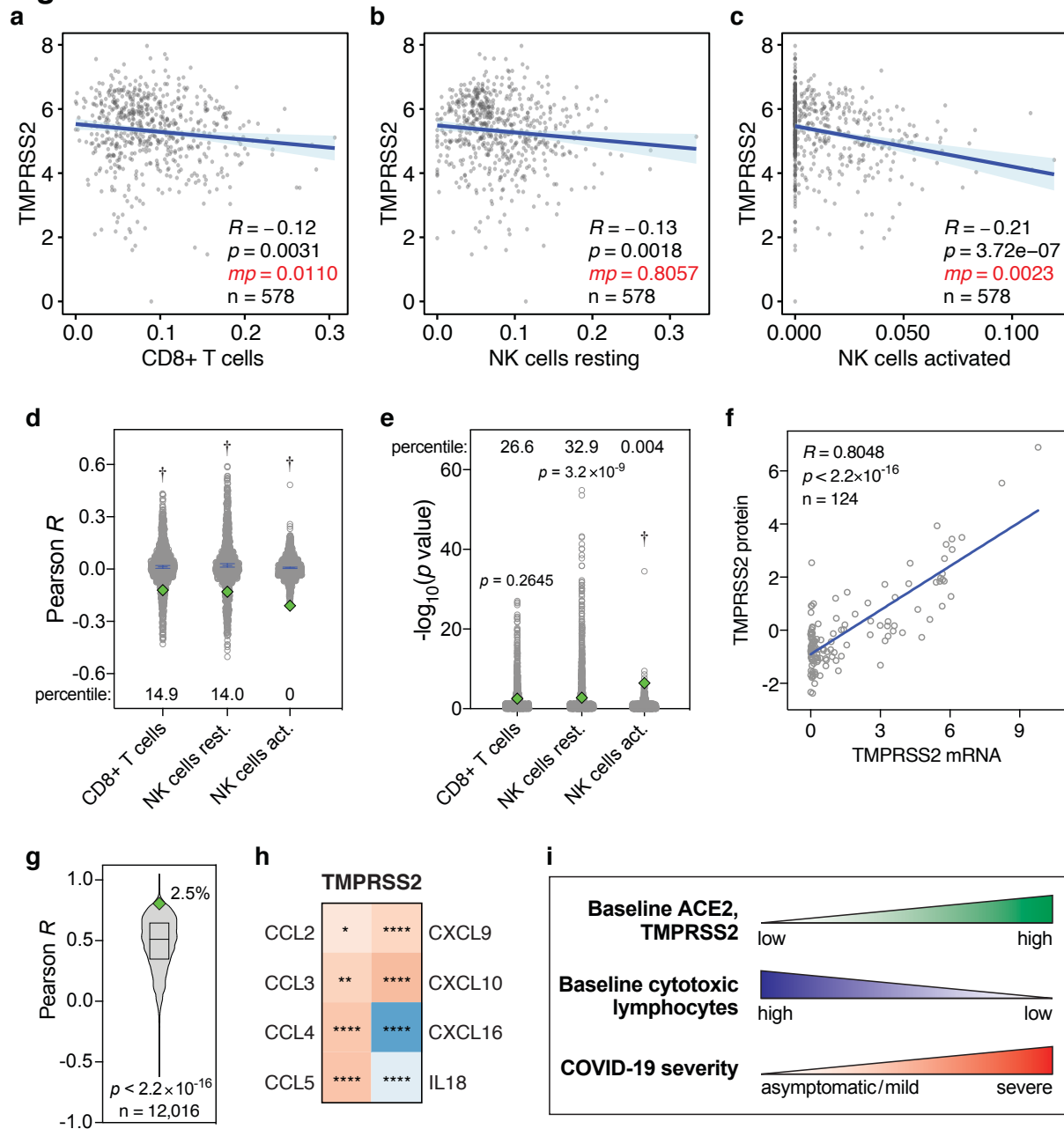


Figure 3. Levels of TMPRSS2 mRNA, TMPRSS2 protein and cytokines in lung cells and tissues. (a-c) Pearson correlations between baseline levels of indicated lymphocytes and TMPRSS2 in human lung tissue, as Figure 1a-c. Data are from the GTEx dataset ($n=578$). (d, e) Pearson R and $-\log_{10}(p \text{ values})$ of correlations between 1000 randomly sampled genes and the levels of indicated lymphocytes in lung tissues, as in Figure 2a,b. TMPRSS2 Pearson R and p values are shown as green diamonds. (f) Correlations between TMPRSS2 mRNA and protein levels in 124 cell lines. R and p values: Pearson correlations. (g) Pearson correlation R values between mRNA and protein levels of 12,016 genes are compared to the TMPRSS2 R coefficient (green diamond). The box represents the median and interquartile range. The TMPRSS2 R percentile is also shown. P value: one-sample t test. (h) Heatmap showing Spearman correlations between the levels of TMPRSS2 and cytokines in human lung tissues from the GTEx dataset ($n=578$), as in Figure 2h. (i) Individuals with high baseline levels of ACE2 and TMPRSS2 show low baseline tissue-resident levels of cytotoxic lymphocytes in the lung. We propose that this may jointly predispose these individuals to development of severe COVID-19.

Supplementary Information

Low baseline pulmonary levels of cytotoxic lymphocytes as a predisposing risk factor for severe COVID-19

Pascal H.G. Duijf

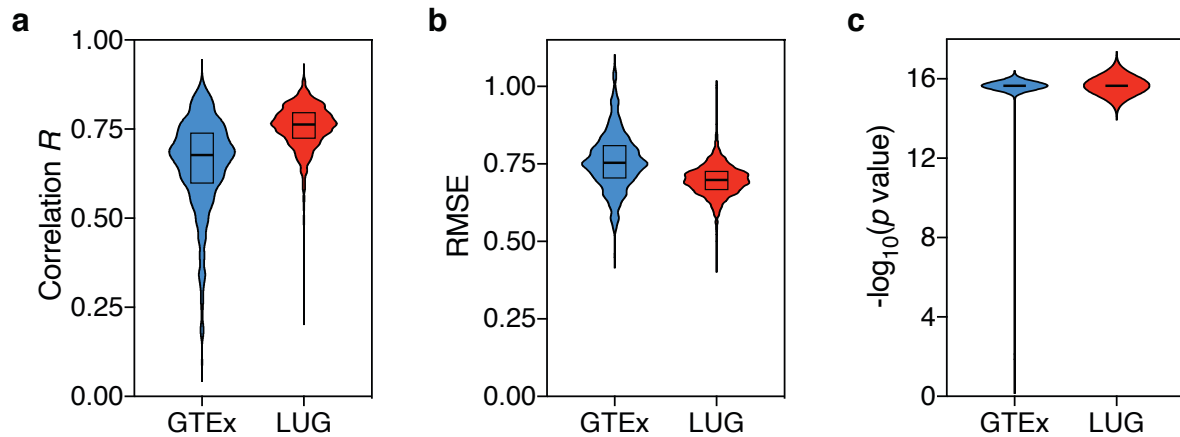


Figure S1. *In silico* cytometry statistics.

Per-sample statistics of *in silico* cytometry on human lung tissues are shown for the GTEx (n=578) and LUG (n=1,349) datasets. (a) Pearson correlation coefficients R . (b) Root mean square errors (RMSE). (c) p values. P values $< 2.2 \times 10^{-16}$ were processed as equal to 2.2×10^{-16} . Source data are provided in Table S1.

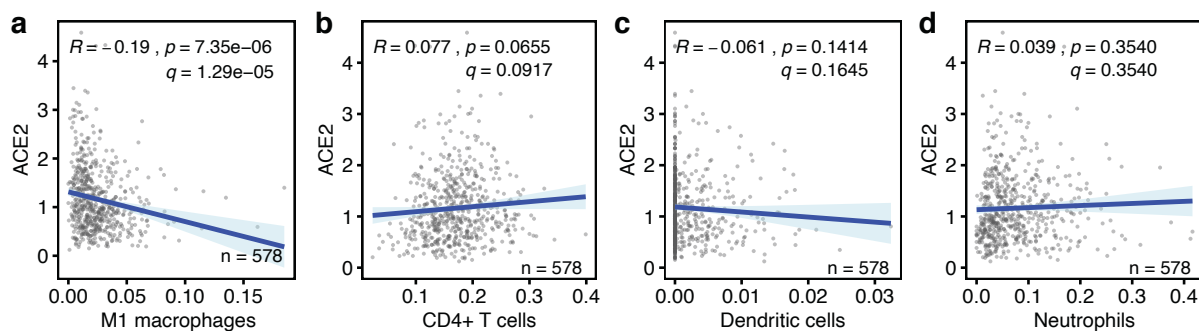


Figure S2. Correlations between baseline anti-viral leukocyte levels and ACE2 expression levels in human lung tissues.

(a-d) The correlations between the baseline levels of indicated immune cell types (x-axes) and the expression level of the SARS-CoV-2 host cell receptor ACE2 (y-axis) in human lung tissue are shown. Data are from the GTEx dataset (n=578). Regression lines and 95% confidence intervals are shown. R and p values: Pearson correlations; q values: Benjamini-Hochberg-adjusted p values using a false discovery rate of 0.05. See also Figure 1.

Figure S3. Correlation between baseline M1 macrophage levels and ACE2 expression level in human lung tissue.

The correlation between these variables is shown as described in Figure S2. Data are from the LUG dataset (n=1,349).

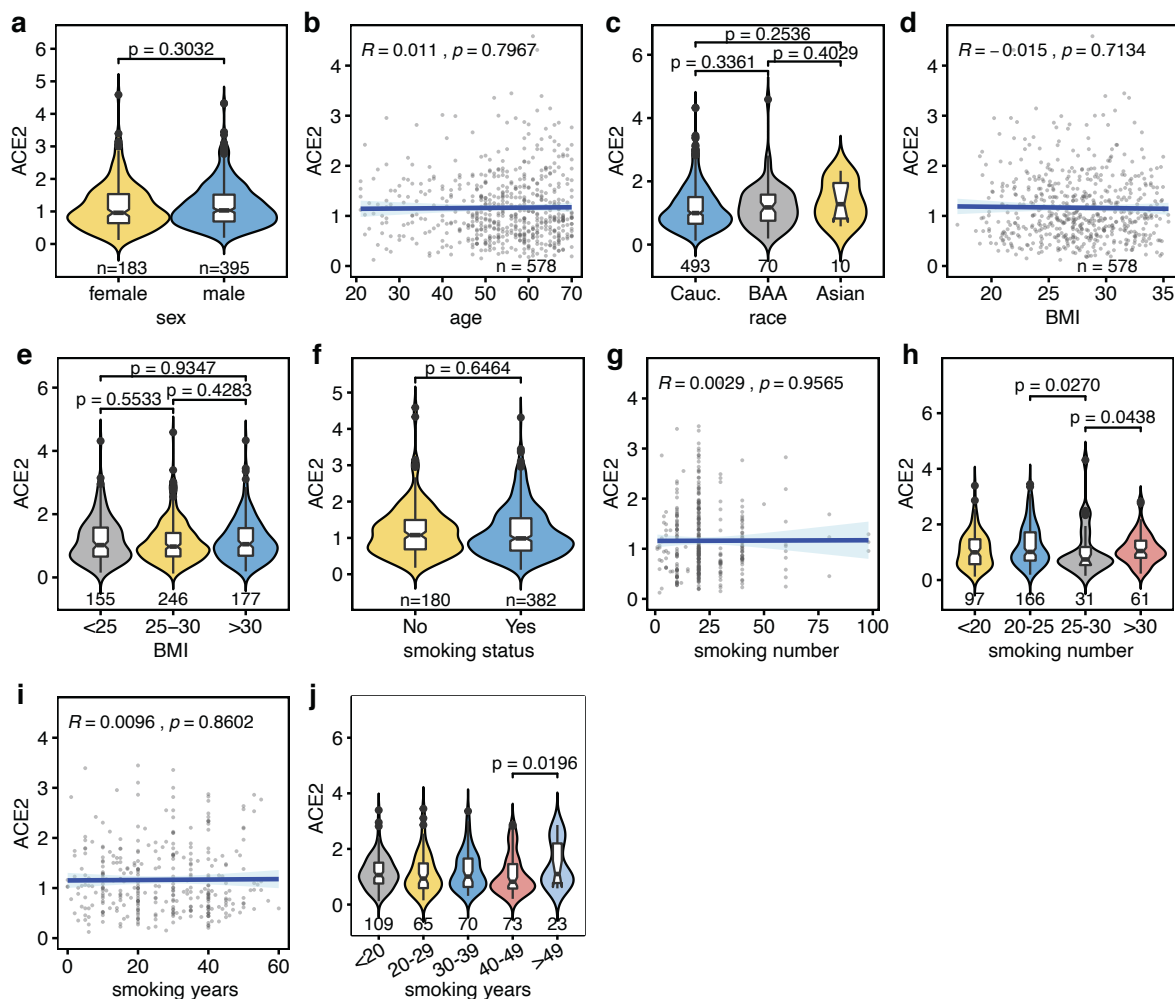
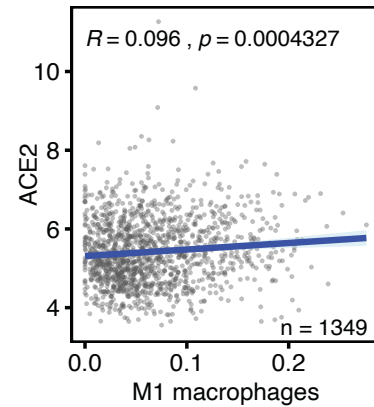


Figure S4. Univariate analyses of phenotypic covariates included in multivariate analyses.

Univariate analyses of five covariates that were included in multivariate analyses of ACE2 and TMPRSS2 expression in human lung tissue using the GTEx dataset (Tables S2, S3). (a) Sex. (b) Age, (c) Race. (d, e) Body mass index. (f-j) Smoking behavior, referring to smoking status (smoker/non-smoker) (f), number of units smoked during the smoke period (g, h) and number of years smoked (i, j). *P* values in categorical analyses: Mann-Whitney *U* tests. *R* and *p* values in continuous analyses: Pearson correlations. *P* values in panels h and j are only shown if *p*<0.05. Sample numbers (*n*) are shown on the x-axes.

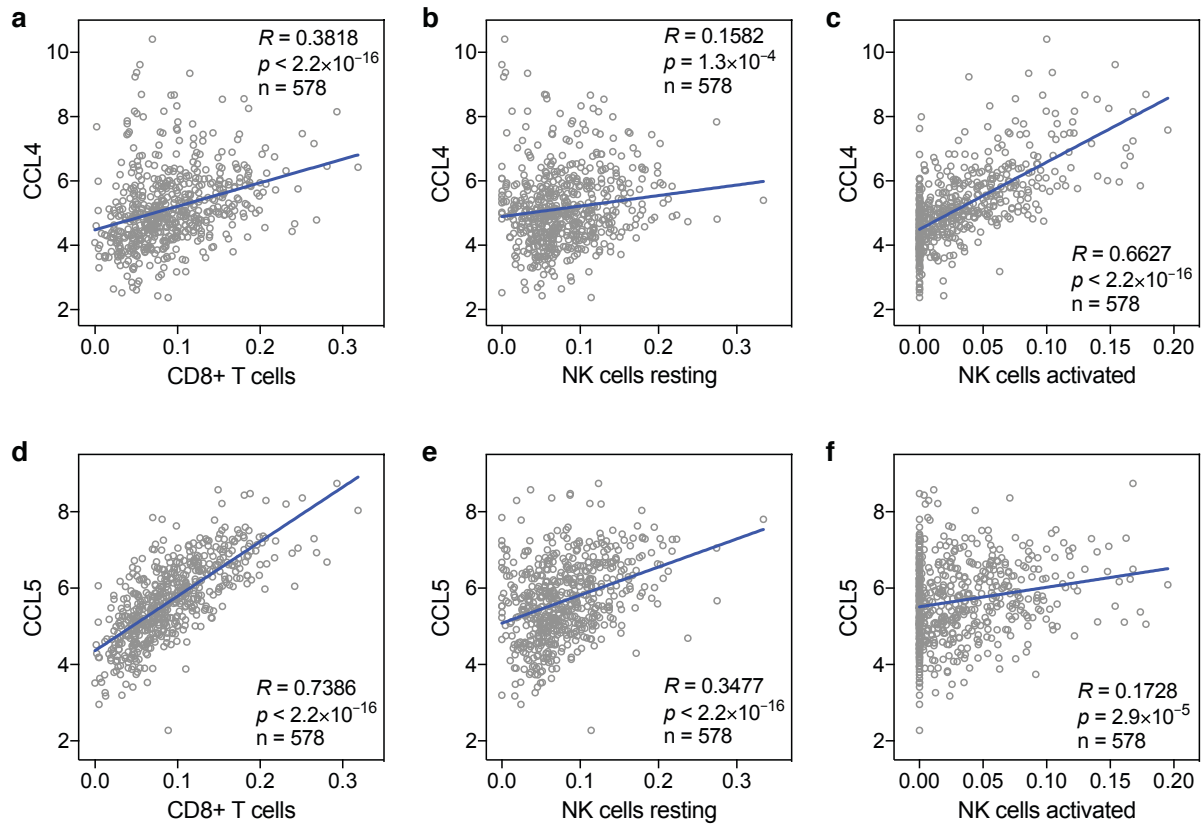


Figure S5. Correlations between baseline levels of cytotoxic lymphocytes and CCL4 and CCL5 in human lung tissue.

The correlations between baseline levels of the chemokines CCL4, CCL5 and CD8+ T cells, resting and activated NK cells in human lung tissue are shown. Data are from the GTEx dataset (n=578). *R* and *p* values: Spearman correlations. See also Figure 2g.

Table S1. Source data of *in silico* cytometry statistics

For each sample in the GTE_x (n=578) and LUG (n=1,349) datasets, Pearson correlation coefficient *R*, root mean square error (RMSE) and $-\log_{10}(p)$ value) are shown. These are the source data of Figure S1.

Sam ple n	GTE _x			LUG			
	GTE _x R	GTE _x RMSE	GTE _x - log ₁₀ pval	LUG R	LUG RMSE	LUG - log ₁₀ pval	
1	0.76787006	0.64982766	15.6575773	0.802959	0.649639	15.65758	
2	0.33960379	0.95534778	15.6575773	0.766379	0.707377	15.65758	
3	0.69311497	0.73304977	15.6575773	0.787641	0.676389	15.65758	
4	0.7996746	0.60995383	15.6575773	0.681417	0.76724	15.65758	
5	0.81489669	0.5873594	15.6575773	0.742665	0.717019	15.65758	
6	0.7328384	0.69463011	15.6575773	0.801268	0.654958	15.65758	
7	0.55167376	0.83420724	15.6575773	0.728905	0.715461	15.65758	
8	0.6898905	0.73547426	15.6575773	0.779413	0.679019	15.65758	
9	0.74337414	0.7268448	15.6575773	0.773965	0.690504	15.65758	
10	0.48677652	0.87413605	15.6575773	0.777735	0.69054	15.65758	
11	0.55088695	0.83618046	15.6575773	0.789392	0.682538	15.65758	
12	0.72198448	0.72751001	15.6575773	0.747533	0.711919	15.65758	
13	0.44847706	0.89376979	15.6575773	0.842775	0.586167	15.65758	
14	0.70299836	0.72682982	15.6575773	0.761953	0.700298	15.65758	
15	0.743309	0.70328228	15.6575773	0.753612	0.708944	15.65758	
16	0.62707528	0.79388999	15.6575773	0.804003	0.657556	15.65758	
17	0.65149292	0.77493294	15.6575773	0.810269	0.653416	15.65758	
18	0.71063774	0.74524749	15.6575773	0.771608	0.701303	15.65758	
19	0.61600528	0.8063179	15.6575773	0.797468	0.669538	15.65758	
20	0.53761731	0.84298471	15.6575773	0.757637	0.707872	15.65758	
21	0.61042154	0.79213496	15.6575773	0.706046	0.744027	15.65758	
22	0.76173265	0.68612869	15.6575773	0.757324	0.704732	15.65758	
23	0.59234111	0.81590966	15.6575773	0.788137	0.684214	15.65758	
24	0.57111551	0.82945874	15.6575773	0.758922	0.67449	15.65758	
25	0.70245483	0.74771223	15.6575773	0.800876	0.675024	15.65758	
26	0.71931585	0.70114944	15.6575773	0.748056	0.717971	15.65758	
27	0.67884846	0.74083394	15.6575773	0.739715	0.723634	15.65758	
28	0.7007555	0.72235034	15.6575773	0.780562	0.674622	15.65758	
29	0.72923843	0.71907274	15.6575773	0.782376	0.682771	15.65758	
30	0.55756861	0.82973695	15.6575773	0.726186	0.73166	15.65758	
31	0.62325326	0.79139104	15.6575773	0.813847	0.649338	15.65758	
32	0.63886768	0.77930992	15.6575773	0.805055	0.660688	15.65758	
33	0.44888773	0.89528101	15.6575773	0.736178	0.715388	15.65758	
34	0.68212751	0.74938995	15.6575773	0.811061	0.663174	15.65758	
35	0.73205242	0.68283704	15.6575773	0.68782	0.758606	15.65758	
36	0.68262106	0.75168703	15.6575773	0.819304	0.652341	15.65758	
37	0.48008816	0.88349271	15.6575773	0.762902	0.701996	15.65758	
38	0.45440411	0.89026941	15.6575773	0.685527	0.761058	15.65758	
39	0.60434542	0.79776549	15.6575773	0.768102	0.690433	15.65758	
40	0.82054193	0.57404279	15.6575773	0.835847	0.617019	15.65758	
41	0.69813151	0.75070076	15.6575773	0.835447	0.633442	15.65758	
42	0.62125354	0.78878221	15.6575773	0.774305	0.690438	15.65758	
43	0.75157392	0.68798327	15.6575773	0.821192	0.634717	15.65758	
44	0.38777408	0.92960941	15.6575773	0.736161	0.721822	15.65758	
45	0.82524164	0.63701517	15.6575773	0.774914	0.694771	15.65758	
46	0.51701022	0.86026052	15.6575773	0.817019	0.65777	15.65758	
47	0.56007914	0.83677468	15.6575773	0.8374	0.597228	15.65758	
48	0.71308175	0.70717759	15.6575773	0.763472	0.70808	15.65758	
49	0.62706859	0.79677808	15.6575773	0.723793	0.732254	15.65758	
50	0.71172223	0.74130879	15.6575773	0.840075	0.586469	15.65758	
51	0.77950068	0.64522993	15.6575773	0.780776	0.690774	15.65758	
52	0.68360264	0.74101263	15.6575773	0.781202	0.687471	15.65758	
53	0.84172362	0.62704355	15.6575773	0.784475	0.654003	15.65758	
54	0.31660643	0.95729498	15.6575773	0.796829	0.669602	15.65758	
55	0.68785982	0.75314287	15.6575773	0.700059	0.745584	15.65758	
56	0.70464449	0.74925695	15.6575773	0.795957	0.679328	15.65758	
57	0.70970752	0.74479217	15.6575773	0.823785	0.631725	15.65758	
58	0.62238904	0.79602679	15.6575773	0.793232	0.683047	15.65758	
59	0.52698581	0.84930394	15.6575773	0.819992	0.644026	15.65758	
60	0.73123587	0.70101211	15.6575773	0.749767	0.699034	15.65758	
61	0.7674915	0.70041919	15.6575773	0.727959	0.726711	15.65758	
62	0.62789934	0.78044364	15.6575773	0.770688	0.703886	15.65758	
63	0.60410025	0.80136883	15.6575773	0.737926	0.714894	15.65758	
64	0.57227658	0.82550032	15.6575773	0.749034	0.706154	15.65758	
65	0.76991092	0.65403992	15.6575773	0.746872	0.711799	15.65758	
66	0.68588497	0.73930282	15.6575773	0.742272	0.717509	15.65758	
67	0.60545218	0.80540731	15.6575773	0.693004	0.74553	15.65758	
68	0.72715468	0.70593705	15.6575773	0.725727	0.725521	15.65758	
69	0.82942443	0.63454869	15.6575773	0.805247	0.660876	15.65758	
70	0.71425946	0.7176295	15.6575773	0.825733	0.620069	15.65758	
71	0.77765493	0.66701741	15.6575773	0.766407	0.69845	15.65758	
72	0.70485216	0.71288925	15.6575773	0.738098	0.727688	15.65758	
73	0.70049108	0.72082562	15.6575773	0.761357	0.701782	15.65758	
74	0.49294211	0.87118578	15.6575773	0.772676	0.688762	15.65758	
75	0.74102721	0.69347067	15.6575773	0.738963	0.717142	15.65758	
76	0.68292334	0.74742974	15.6575773	0.820638	0.654015	15.65758	
77	0.68202831	0.74271381	15.6575773	0.804679	0.677565	15.65758	
78	0.66058818	0.77004578	15.6575773	0.814325	0.667653	15.65758	
79	0.61258367	0.79117276	15.6575773	0.715896	0.727023	15.65758	
80	0.66021942	0.76245576	15.6575773	0.757175	0.711845	15.65758	
81	0.73545094	0.70171276	15.6575773	0.745553	0.71137	15.65758	
82	0.76539688	0.70190687	15.6575773	0.812	0.653151	15.65758	
83	0.52249671	0.85192189	15.6575773	0.747185	0.716424	15.65758	
84	0.50301948	0.86526106	15.6575773	0.803403	0.669913	15.65758	
85	0.51410756	0.85722208	15.6575773	0.789727	0.672406	15.65758	
86	0.54248051	0.84295889	15.6575773	0.672214	0.76654	15.65758	
87	0.54325456	0.83888963	15.6575773	0.705861	0.743058	15.65758	
88	0.67174415	0.7604468	15.6575773	0.704747	0.743665	15.65758	
89	0.19835402	1.04850401	2	0.804903	0.650558	15.65758	
90	0.80546361	0.6228925	15.6575773	0.6228925	0.774205	0.670835	15.65758
91	0.77078186	0.66191298	15.6575773	0.66191298	0.733251	0.716882	15.65758
92	0.61667107	0.80159867	15.6575773	0.80159867	0.756188	0.711612	15.65758
93	0.6965581	0.72055837	15.6575773	0.72055837	0.799211	0.669125	15.65758
94	0.72414493	0.69095633	15.6575773	0.69095633	0.775547	0.686414	15.65758
95	0.56751768	0.82297723	15.6575773	0.82297723	0.771394	0.687734	15.65758
96	0.68384218	0.7419826	15.6575773	0.7419826	0.772536	0.694775	15.65758
97	0.55867087	0.83016121	15.6575773	0.83016121	0.739445	0.719632	15.65758
98	0.59189641	0.80927822	15.6575773	0.80927822	0.731612	0.725989	15.65758
99	0.66689221	0.74551067	15.6575773	0.74551067	0.762586	0.705917	15.65758
100	0.76408857	0.68936908	15.6575773	0.68936908	0.755818	0.682473	15.65758
101	0.78195749	0.65704796	15.6575773	0.65704796	0.781971	0.6349	15.65758
102	0.62157124	0.79616277	15.6575773	0.79616277	0.782796	0.679205	15.65758
103	0.69262931	0.73158418	15.6575773	0.73158418	0.711814	0.741561	15.65758
104	0.35999342	0.93722591	15.6575773	0.93722591	0.830347	0.667358	15.65758
105	0.57105776	0.82676047	15.6575773	0.82676047	0.742403	0.721198	15.65758
106	0.61157077	0.79751651	15.6575773	0.79751651	0.8256	0.632411	15.65758
107	0.62836027	0.78725474	15.6575773	0.78725474	0.723734	0.72605	15.65758
108	0.63730953	0.77172128	15.6575773	0.77172128	0.676773	0.758942	15.65758
109	0.55034452	0.8364782	15.6575773	0.8364782	0.788154	0.685592	15.65758
110	0.58071617	0.81963676	15.6575773	0.81963676	0.841142	0.578848	15.65758
111	0.64288144	0.76919284	15.6575773	0.76919284	0.74721	0.712274	15.65758
112	0.76962275	0.6741102	15.6575773	0.6741102	0.779528	0.681984	15.65758
113	0.74316718	0.6962846	15.6575773	0.6962846	0.815183	0.62824	15.65758
114	0.74932054	0.7188616	15.6575773	0.7188616	0.7221	0.740452	15.65758
115	0.70768548	0.7150471	15.6575773	0.7150471	0.74199	0.71447	15.65758
116	0.64318529	0.77146204	15.6575773	0.77146204	0.747192	0.711697	15.65758
117	0.50027396	0.86654572	15.6575773	0.86654572	0.76586	0.700596	15.65758
118	0.62888656	0.7635483	15.6575773	0.7635483	0.797885	0.666194	15.65758
119	0.5870206	0.81213873	15.6575773	0.81213873	0.798512	0.671222	15.65758
1							

193	0.72599161	0.74095472	15.657573	0.7571	0.715478	15.657578
194	0.66043078	0.75296204	15.657573	0.75468	0.709712	15.657578
195	0.56001772	0.83338094	15.657573	0.716521	0.732976	15.657578
196	0.81838675	0.60658809	15.657573	0.821864	0.636654	15.657578
197	0.77302519	0.63590636	15.657573	0.647836	0.784919	15.657578
198	0.54390926	0.84098442	15.657573	0.747368	0.708886	15.657578
199	0.67961129	0.75558107	15.657573	0.763616	0.689703	15.657578
200	0.60649215	0.7960565	15.657573	0.812353	0.6419	15.657578
201	0.48456997	0.87433601	15.657573	0.79388	0.651875	15.657578
202	0.81596176	0.64460334	15.657573	0.761849	0.690674	15.657578
203	0.74966186	0.66777995	15.657573	0.781606	0.663368	15.657578
204	0.75464334	0.65831696	15.657573	0.821076	0.660814	15.657578
205	0.74968041	0.72670082	15.657573	0.796044	0.666209	15.657578
206	0.81399703	0.58351606	15.657573	0.791838	0.680987	15.657578
207	0.68506628	0.75996461	15.657573	0.789881	0.689701	15.657578
208	0.6360702	0.78975549	15.657573	0.809869	0.647442	15.657578
209	0.58242464	0.81682636	15.657573	0.724377	0.731891	15.657578
210	0.68684771	0.75712965	15.657573	0.804232	0.607361	15.657578
211	0.75432658	0.70731847	15.657573	0.772383	0.700347	15.657578
212	0.74763336	0.70352207	15.657573	0.79732	0.668725	15.657578
213	0.7345029	0.6906848	15.657573	0.820374	0.643138	15.657578
214	0.38555341	0.92473625	15.657573	0.786387	0.671845	15.657578
215	0.66480243	0.77317655	15.657573	0.722954	0.725167	15.657578
216	0.53238055	0.8501063	15.657573	0.661335	0.76966	15.657578
217	0.49614753	0.87117367	15.657573	0.747917	0.713147	15.657578
218	0.62848809	0.78155805	15.657573	0.754777	0.713618	15.657578
219	0.34756065	0.9461676	15.657573	0.812003	0.672584	15.657578
220	0.71911963	0.70564645	15.657573	0.752694	0.706264	15.657578
221	0.59834917	0.81128019	15.657573	0.790308	0.685963	15.657578
222	0.47498616	0.87943216	15.657573	0.836905	0.637796	15.657578
223	0.60689839	0.79634132	15.657573	0.799052	0.669879	15.657578
224	0.50019681	0.86724432	15.657573	0.793398	0.663917	15.657578
225	0.62729209	0.79058412	15.657573	0.781364	0.688733	15.657578
226	0.46225126	0.88865426	15.657573	0.780071	0.690821	15.657578
227	0.67231135	0.76832341	15.657573	0.787926	0.675839	15.657578
228	0.64748332	0.76768051	15.657573	0.82181	0.631713	15.657578
229	0.62251406	0.78420097	15.657573	0.843974	0.604237	15.657578
230	0.8183653	0.67757687	15.657573	0.731429	0.728452	15.657578
231	0.75270747	0.71496551	15.657573	0.763006	0.705997	15.657578
232	0.6068207	0.79963664	15.657573	0.74788	0.711903	15.657578
233	0.58879924	0.8080764	15.657573	0.750129	0.707874	15.657578
234	0.19851404	1.02630196	2	0.796418	0.649542	15.657578
235	0.71390061	0.74582221	15.657573	0.719688	0.729439	15.657578
236	0.76283788	0.68148595	15.657573	0.76701	0.698827	15.657578
237	0.60732441	0.79707316	15.657573	0.557045	0.836521	15.657578
238	0.54137454	0.84031461	15.657573	0.786279	0.675397	15.657578
239	0.57237844	0.82061417	15.657573	0.772489	0.694027	15.657578
240	0.89292037	0.45411744	15.657573	0.791821	0.645896	15.657578
241	0.65583111	0.75916878	15.657573	0.725282	0.728549	15.657578
242	0.774149	0.70954979	15.657573	0.835758	0.615321	15.657578
243	0.67806547	0.76133731	15.657573	0.749561	0.716408	15.657578
244	0.49364517	0.86885487	15.657573	0.667615	0.773075	15.657578
245	0.536933	0.84322847	15.657573	0.765581	0.683119	15.657578
246	0.70872418	0.7076122	15.657573	0.734532	0.72122	15.657578
247	0.77589014	0.67296294	15.657573	0.674216	0.766718	15.657578
248	0.80072619	0.61393943	15.657573	0.803479	0.666537	15.657578
249	0.65988256	0.77526385	15.657573	0.787501	0.678435	15.657578
250	0.68068467	0.74091501	15.657573	0.76172	0.703398	15.657578
251	0.73244551	0.70928926	15.657573	0.795979	0.678793	15.657578
252	0.75354693	0.67422913	15.657573	0.776025	0.688462	15.657578
253	0.63254677	0.79478404	15.657573	0.798442	0.680254	15.657578
254	0.6153526	0.79113624	15.657573	0.738534	0.71802	15.657578
255	0.56034604	0.82753621	15.657573	0.787161	0.676819	15.657578
256	0.77369824	0.65969904	15.657573	0.744086	0.717224	15.657578
257	0.85411372	0.56176758	15.657573	0.786093	0.66527	15.657578
258	0.57687458	0.81685974	15.657573	0.801868	0.644505	15.657578
259	0.69854543	0.73007923	15.657573	0.735325	0.72027	15.657578
260	0.26945451	0.97889818	15.657573	0.820929	0.652595	15.657578
261	0.84318789	0.58198357	15.657573	0.742597	0.714365	15.657578
262	0.69618896	0.75954336	15.657573	0.81396	0.632136	15.657578
263	0.44164111	0.8971177	15.657573	0.825774	0.638587	15.657578
264	0.63749278	0.78479043	15.657573	0.705999	0.744879	15.657578
265	0.86949088	0.57450335	15.657573	0.817806	0.658609	15.657578
266	0.8281639	0.5636942	15.657573	0.768556	0.680677	15.657578
267	0.66002965	0.75860091	15.657573	0.7489624	0.608813	15.657578
268	0.75685307	0.71151029	15.657573	0.737617	0.723191	15.657578
269	0.57332907	0.82288263	15.657573	0.710483	0.723503	15.657578
270	0.84539899	0.59464806	15.657573	0.784225	0.68118	15.657578
271	0.76104507	0.65077789	15.657573	0.728	0.728922	15.657578
272	0.6640011	0.76063509	15.657573	0.740465	0.716417	15.657578
273	0.66142851	0.75573128	15.657573	0.792563	0.679577	15.657578
274	0.09561775	1.06392067	0.92081875	0.804311	0.656906	15.657578
275	0.59691428	0.81195173	15.657573	0.764963	0.695617	15.657578
276	0.66214351	0.77044357	15.657573	0.796255	0.672442	15.657578
277	0.77865783	0.65298519	15.657573	0.827325	0.657303	15.657578
278	0.54618294	0.84078972	15.657573	0.662821	0.768781	15.657578
279	0.6933973	0.73413878	15.657573	0.762835	0.700561	15.657578
280	0.68076046	0.7351417	15.657573	0.751751	0.695009	15.657578
281	0.64173496	0.7808481	15.657573	0.738474	0.711002	15.657578
282	0.62576569	0.80111043	15.657573	0.816107	0.653323	15.657578
283	0.7198404	0.69761934	15.657573	0.775223	0.682029	15.657578
284	0.55056818	0.83413069	15.657573	0.836076	0.628891	15.657578
285	0.70713266	0.71949422	15.657573	0.751681	0.701574	15.657578
286	0.42489912	0.90477606	15.657573	0.783174	0.692962	15.657578
287	0.731716	0.71285487	15.657573	0.768599	0.690812	15.657578
288	0.81458549	0.62653519	15.657573	0.741483	0.706972	15.657578
289	0.66883619	0.74993247	15.657573	0.779969	0.693146	15.657578
290	0.59842802	0.80157266	15.657573	0.68451	0.759285	15.657578
291	0.65410643	0.77468509	15.657573	0.818814	0.645443	15.657578
292	0.71982128	0.70302377	15.657573	0.748352	0.713861	15.657578
293	0.84054467	0.58340764	15.657573	0.772643	0.689538	15.657578
294	0.65200613	0.78014444	15.657573	0.682554	0.758181	15.657578
295	0.43740953	0.8993488	15.657573	0.764508	0.673325	15.657578
296	0.69769203	0.74067558	15.657573	0.73447	0.722677	15.657578
297	0.62942763	0.79526233	15.657573	0.709712	0.722765	15.657578
298	0.34273059	0.95188053	15.657573	0.757274	0.714485	15.657578
299	0.86048091	0.54256793	15.657573	0.841756	0.592278	15.657578
300	0.61614358	0.79170506	15.657573	0.800507	0.654171	15.657578
301	0.67335919	0.75445336	15.657573	0.770732	0.701699	15.657578
302	0.35345743	0.94275013	15.657573	0.767875	0.698409	15.657578
303	0.71042911	0.74494089	15.657573	0.767138	0.701982	15.657578
304	0.8477898	0.53334989	15.657573	0.864484	0.58774	15.657578
305	0.67903314	0.73579422	15.657573	0.731853	0.725057	15.657578
306	0.63074111	0.79044464	15.657573	0.737426	0.715749	15.657578
307	0.64005978	0.78176292	15.657573	0.77896	0.686587	15.657578
308	0.66719365	0.75715937	15.657573	0.671694	0.759826	15.657578
309	0.68957512	0.75765528	15.657573	0.753052	0.716508	15.657578
310	0.48493149	0.88565917	15.657573	0.756836	0.700051	15.657578
311	0.39856453	0.92223475	15.657573	0.758049	0.707652	15.657578
312	0.78137492	0.66483924	15.657573	0.790423	0.68897	15.657578
313	0.78942621	0.64359881	15.657573	0.814714	0.667971	15.657578
314	0.76627041	0.66710032	15.657573	0.824011	0.654317	15.657578
315	0.825058	0.58586794	15.657573	0.811953	0.63457	15.657578
316	0.69565437	0.72924025	15.657573	0.736519	0.721321	15.657578
317	0.61540866	0.79928767	15.657573	0.817248	0.628069	15.657578
318	0.67771209	0.75088031	15.657573	0.70467	0.746934	15.657578
319	0.52363313	0.85124364	15.657573	0.75058	0.71488	15.657578
320	0.87085539	0.54369011	1			

605	0.836401	0.628687	15.65758	708	0.687113	0.751077	15.65758
606	0.911251	0.419262	15.65758	709	0.775649	0.668987	15.65758
607	0.818817	0.6423	15.65758	710	0.73186	0.728451	15.65758
608	0.815959	0.587867	15.65758	711	0.794779	0.668587	15.65758
609	0.775377	0.701169	15.65758	712	0.746058	0.714136	15.65758
610	0.810637	0.676703	15.65758	713	0.783579	0.684422	15.65758
611	0.783418	0.686293	15.65758	714	0.793903	0.623058	15.65758
612	0.827488	0.651619	15.65758	715	0.797154	0.644642	15.65758
613	0.830243	0.633429	15.65758	716	0.829359	0.654034	15.65758
614	0.76299	0.706539	15.65758	717	0.794461	0.67782	15.65758
615	0.777326	0.683108	15.65758	718	0.746753	0.713377	15.65758
616	0.792992	0.688547	15.65758	719	0.764302	0.709912	15.65758
617	0.791698	0.667083	15.65758	720	0.821783	0.669849	15.65758
618	0.746328	0.709129	15.65758	721	0.600036	0.803218	15.65758
619	0.824635	0.653013	15.65758	722	0.773492	0.697938	15.65758
620	0.780386	0.695657	15.65758	723	0.748952	0.708535	15.65758
621	0.890327	0.548828	15.65758	724	0.802202	0.669293	15.65758
622	0.765789	0.695786	15.65758	725	0.872055	0.608634	15.65758
623	0.793323	0.67593	15.65758	726	0.821294	0.652607	15.65758
624	0.799253	0.685113	15.65758	727	0.726352	0.722836	15.65758
625	0.707269	0.713864	15.65758	728	0.659818	0.765166	15.65758
626	0.815809	0.659695	15.65758	729	0.782503	0.684321	15.65758
627	0.756838	0.708618	15.65758	730	0.688529	0.744634	15.65758
628	0.758913	0.712994	15.65758	731	0.773486	0.705232	15.65758
629	0.806806	0.670664	15.65758	732	0.691429	0.749325	15.65758
630	0.725551	0.702166	15.65758	733	0.71483	0.729752	15.65758
631	0.789219	0.677406	15.65758	734	0.78104	0.684301	15.65758
632	0.798177	0.671401	15.65758	735	0.75907	0.690635	15.65758
633	0.771027	0.67813	15.65758	736	0.610114	0.800979	15.65758
634	0.809229	0.666031	15.65758	737	0.756082	0.695542	15.65758
635	0.752316	0.7117	15.65758	738	0.76771	0.686997	15.65758
636	0.745579	0.711261	15.65758	739	0.804666	0.665904	15.65758
637	0.745375	0.717513	15.65758	740	0.664061	0.753398	15.65758
638	0.828201	0.622256	15.65758	741	0.810006	0.663316	15.65758
639	0.819101	0.644291	15.65758	742	0.749778	0.721999	15.65758
640	0.783208	0.690717	15.65758	743	0.810336	0.665186	15.65758
641	0.639238	0.786195	15.65758	744	0.712186	0.735793	15.65758
642	0.728835	0.728735	15.65758	745	0.783865	0.679325	15.65758
643	0.5941	0.810263	15.65758	746	0.796486	0.682023	15.65758
644	0.743587	0.716656	15.65758	747	0.796407	0.671123	15.65758
645	0.819951	0.659432	15.65758	748	0.804208	0.675282	15.65758
646	0.71859	0.736019	15.65758	749	0.800447	0.654541	15.65758
647	0.817048	0.659215	15.65758	750	0.767746	0.693829	15.65758
648	0.814462	0.666707	15.65758	751	0.732253	0.728506	15.65758
649	0.737011	0.71207	15.65758	752	0.751563	0.699475	15.65758
650	0.751921	0.716585	15.65758	753	0.81538	0.675123	15.65758
651	0.771256	0.690252	15.65758	754	0.823838	0.657871	15.65758
652	0.779024	0.688401	15.65758	755	0.758944	0.710429	15.65758
653	0.784727	0.669316	15.65758	756	0.695817	0.739976	15.65758
654	0.763146	0.688507	15.65758	757	0.826663	0.628033	15.65758
655	0.761684	0.700649	15.65758	758	0.853517	0.595221	15.65758
656	0.744078	0.718388	15.65758	759	0.797715	0.681695	15.65758
657	0.839238	0.631888	15.65758	760	0.785589	0.691973	15.65758
658	0.712365	0.70875	15.65758	761	0.795076	0.679921	15.65758
659	0.781958	0.696883	15.65758	762	0.768809	0.719103	15.65758
660	0.764964	0.708114	15.65758	763	0.84491	0.646007	15.65758
661	0.781655	0.694766	15.65758	764	0.773846	0.684647	15.65758
662	0.88273	0.513199	15.65758	765	0.84135	0.614592	15.65758
663	0.708519	0.743325	15.65758	766	0.808888	0.672955	15.65758
664	0.78099	0.685178	15.65758	767	0.782672	0.682618	15.65758
665	0.705255	0.723169	15.65758	768	0.7018	0.747612	15.65758
666	0.78502	0.685646	15.65758	769	0.820353	0.624411	15.65758
667	0.696065	0.734747	15.65758	770	0.763721	0.692248	15.65758
668	0.832355	0.645889	15.65758	771	0.770611	0.680024	15.65758
669	0.687384	0.756173	15.65758	772	0.725137	0.731628	15.65758
670	0.778759	0.689232	15.65758	773	0.739857	0.718038	15.65758
671	0.739144	0.727058	15.65758	774	0.855136	0.583444	15.65758
672	0.766936	0.700403	15.65758	775	0.752022	0.712958	15.65758
673	0.831052	0.656697	15.65758	776	0.736903	0.721651	15.65758
674	0.76816	0.703657	15.65758	777	0.793606	0.622588	15.65758
675	0.80481	0.656479	15.65758	778	0.822497	0.644963	15.65758
676	0.830248	0.662945	15.65758	779	0.825582	0.619915	15.65758
677	0.799644	0.675043	15.65758	780	0.772236	0.692406	15.65758
678	0.755421	0.682801	15.65758	781	0.791914	0.653098	15.65758
679	0.807969	0.663481	15.65758	782	0.808445	0.672087	15.65758
680	0.778601	0.703357	15.65758	783	0.793581	0.687456	15.65758
681	0.678404	0.759408	15.65758	784	0.679075	0.760631	15.65758
682	0.844275	0.562663	15.65758	785	0.775771	0.674573	15.65758
683	0.771829	0.692486	15.65758	786	0.855273	0.603479	15.65758
684	0.827057	0.658848	15.65758	787	0.766861	0.699522	15.65758
685	0.8889	0.520816	15.65758	788	0.833812	0.63632	15.65758
686	0.779557	0.685926	15.65758	789	0.671904	0.767981	15.65758
687	0.826954	0.656704	15.65758	790	0.627788	0.780373	15.65758
688	0.769125	0.699903	15.65758	791	0.691161	0.754252	15.65758
689	0.881961	0.496594	15.65758	792	0.800067	0.633382	15.65758
690	0.710025	0.745151	15.65758	793	0.681481	0.747214	15.65758
691	0.815741	0.637419	15.65758	794	0.896852	0.506732	15.65758
692	0.864562	0.58562	15.65758	795	0.826931	0.646884	15.65758
693	0.731239	0.725962	15.65758	796	0.81027	0.685558	15.65758
694	0.725731	0.733802	15.65758	797	0.833139	0.601492	15.65758
695	0.809398	0.650864	15.65758	798	0.866313	0.595174	15.65758
696	0.844813	0.629186	15.65758	799	0.761802	0.70396	15.65758
697	0.772659	0.696847	15.65758	800	0.708014	0.73629	15.65758
698	0.785803	0.684959	15.65758	801	0.777637	0.693333	15.65758
699	0.875638	0.559683	15.65758	802	0.820679	0.64775	15.65758
700	0.745452	0.708584	15.65758	803	0.783761	0.667992	15.65758
701	0.629989	0.794424	15.65758	804	0.745293	0.71143	15.65758
702	0.814794	0.658299	15.65758	805	0.722151	0.743919	15.65758
703	0.755485	0.715518	15.65758	806	0.761253	0.710745	15.65758
704	0.831513	0.634615	15.65758	807	0.73444	0.683018	15.65758
705	0.852114	0.583726	15.65758	808	0.768755	0.704782	15.65758
706	0.849181	0.608123	15.65758	809	0.746894	0.717701	15.65758
707	0.766739	0.672542	15.65758	810	0.707796	0.743212	15.65758

811		0.691524	0.75594	15.65758	914		0.716453	0.742462	15.65758
812		0.78693	0.666508	15.65758	915		0.654978	0.773194	15.65758
813		0.745628	0.698497	15.65758	916		0.625046	0.795415	15.65758
814		0.74929	0.713002	15.65758	917		0.714263	0.730403	15.65758
815		0.768514	0.698464	15.65758	918		0.770429	0.693096	15.65758
816		0.842632	0.584736	15.65758	919		0.749573	0.693034	15.65758
817		0.7051	0.730224	15.65758	920		0.772131	0.695857	15.65758
818		0.76721	0.699879	15.65758	921		0.766798	0.691671	15.65758
819		0.787893	0.671389	15.65758	922		0.756766	0.698513	15.65758
820		0.780374	0.682974	15.65758	923		0.640414	0.779451	15.65758
821		0.785363	0.692493	15.65758	924		0.750113	0.706342	15.65758
822		0.859342	0.549345	15.65758	925		0.719802	0.728077	15.65758
823		0.767217	0.704088	15.65758	926		0.777063	0.679308	15.65758
824		0.739796	0.720221	15.65758	927		0.663746	0.766772	15.65758
825		0.728577	0.733938	15.65758	928		0.719106	0.712363	15.65758
826		0.733453	0.726341	15.65758	929		0.751487	0.692049	15.65758
827		0.732387	0.72961	15.65758	930		0.790472	0.674228	15.65758
828		0.815105	0.630482	15.65758	931		0.605095	0.802587	15.65758
829		0.839441	0.65636	15.65758	932		0.755214	0.715396	15.65758
830		0.834698	0.650292	15.65758	933		0.697897	0.74966	15.65758
831		0.771269	0.704258	15.65758	934		0.785667	0.692032	15.65758
832		0.789611	0.686827	15.65758	935		0.739355	0.719973	15.65758
833		0.735719	0.72393	15.65758	936		0.741586	0.708798	15.65758
834		0.814591	0.616849	15.65758	937		0.771365	0.688013	15.65758
835		0.790419	0.689815	15.65758	938		0.740556	0.698675	15.65758
836		0.78473	0.682878	15.65758	939		0.696002	0.751329	15.65758
837		0.813936	0.656387	15.65758	940		0.806964	0.656185	15.65758
838		0.829929	0.611358	15.65758	941		0.681813	0.755193	15.65758
839		0.772189	0.694661	15.65758	942		0.668765	0.764835	15.65758
840		0.707238	0.720096	15.65758	943		0.677381	0.757851	15.65758
841		0.685376	0.754889	15.65758	944		0.751058	0.663902	15.65758
842		0.769271	0.691431	15.65758	945		0.732774	0.689789	15.65758
843		0.744316	0.714659	15.65758	946		0.67583	0.757583	15.65758
844		0.880236	0.542133	15.65758	947		0.771558	0.680492	15.65758
845		0.760082	0.702195	15.65758	948		0.697133	0.727558	15.65758
846		0.763591	0.702477	15.65758	949		0.810621	0.659512	15.65758
847		0.809324	0.672497	15.65758	950		0.784512	0.665114	15.65758
848		0.822625	0.612721	15.65758	951		0.840039	0.615174	15.65758
849		0.766008	0.712739	15.65758	952		0.694421	0.744816	15.65758
850		0.785518	0.69913	15.65758	953		0.712999	0.7328	15.65758
851		0.675955	0.765904	15.65758	954		0.838536	0.616874	15.65758
852		0.800859	0.602692	15.65758	955		0.65724	0.771597	15.65758
853		0.858401	0.561668	15.65758	956		0.744268	0.710347	15.65758
854		0.769692	0.692131	15.65758	957		0.729235	0.72432	15.65758
855		0.816124	0.659429	15.65758	958		0.70442	0.729031	15.65758
856		0.771042	0.692388	15.65758	959		0.775332	0.695943	15.65758
857		0.771223	0.686221	15.65758	960		0.630596	0.789718	15.65758
858		0.670844	0.76087	15.65758	961		0.701197	0.723258	15.65758
859		0.737992	0.727044	15.65758	962		0.806464	0.633677	15.65758
860		0.672762	0.762582	15.65758	963		0.703745	0.725434	15.65758
861		0.887975	0.483904	15.65758	964		0.582657	0.822075	15.65758
862		0.73406	0.723293	15.65758	965		0.700899	0.717601	15.65758
863		0.816208	0.655008	15.65758	966		0.696693	0.742772	15.65758
864		0.841274	0.657643	15.65758	967		0.720849	0.714114	15.65758
865		0.799198	0.687463	15.65758	968		0.716702	0.729774	15.65758
866		0.835788	0.629502	15.65758	969		0.756091	0.676041	15.65758
867		0.777863	0.689189	15.65758	970		0.761053	0.694696	15.65758
868		0.695276	0.752255	15.65758	971		0.825623	0.619598	15.65758
869		0.712226	0.736885	15.65758	972		0.760872	0.685556	15.65758
870		0.773715	0.697803	15.65758	973		0.767353	0.701338	15.65758
871		0.79545	0.687114	15.65758	974		0.751818	0.716972	15.65758
872		0.765891	0.688616	15.65758	975		0.672787	0.758048	15.65758
873		0.795922	0.683263	15.65758	976		0.70122	0.735332	15.65758
874		0.769179	0.682906	15.65758	977		0.548242	0.841881	15.65758
875		0.760249	0.70093	15.65758	978		0.653347	0.778939	15.65758
876		0.819652	0.651266	15.65758	979		0.657986	0.758886	15.65758
877		0.70846	0.709759	15.65758	980		0.693729	0.739627	15.65758
878		0.803284	0.649877	15.65758	981		0.75958	0.68512	15.65758
879		0.80757	0.666417	15.65758	982		0.787659	0.682513	15.65758
880		0.775111	0.697829	15.65758	983		0.783072	0.673346	15.65758
881		0.763048	0.704407	15.65758	984		0.852235	0.565936	15.65758
882		0.768287	0.701009	15.65758	985		0.756683	0.704229	15.65758
883		0.767751	0.694695	15.65758	986		0.776682	0.70108	15.65758
884		0.822764	0.634876	15.65758	987		0.744442	0.717364	15.65758
885		0.850516	0.640262	15.65758	988		0.705559	0.729741	15.65758
886		0.591747	0.816696	15.65758	989		0.691645	0.735575	15.65758
887		0.73863	0.725974	15.65758	990		0.766992	0.682072	15.65758
888		0.748382	0.720216	15.65758	991		0.723486	0.723949	15.65758
889		0.804458	0.656342	15.65758	992		0.624424	0.793921	15.65758
890		0.769842	0.692604	15.65758	993		0.224089	1.000564	15.65758
891		0.778384	0.691461	15.65758	994		0.742459	0.701235	15.65758
892		0.728208	0.728898	15.65758	995		0.669515	0.762791	15.65758
893		0.81855	0.672021	15.65758	996		0.800951	0.650713	15.65758
894		0.704846	0.746881	15.65758	997		0.688341	0.743621	15.65758
895		0.72821	0.730615	15.65758	998		0.680654	0.742041	15.65758
896		0.77736	0.658292	15.65758	999		0.750087	0.70924	15.65758
897		0.701517	0.744183	15.65758	1000		0.781958	0.684516	15.65758
898		0.784194	0.643621	15.65758	1001		0.837911	0.624383	15.65758
899		0.802241	0.66083	15.65758	1002		0.771139	0.686127	15.65758
900		0.825347	0.655826	15.65758	1003		0.735688	0.722035	15.65758
901		0.783879	0.671634	15.65758	1004		0.747783	0.686443	15.65758
902		0.812159	0.651685	15.65758	1005		0.727815	0.690349	15.65758
903		0.787115	0.68212	15.65758	1006		0.762345	0.700186	15.65758
904		0.765787	0.695202	15.65758	1007		0.718939	0.72389	15.65758
905		0.789955	0.691247	15.65758	1008		0.746073	0.719766	15.65758
906		0.743388	0.691064	15.65758	1009		0.705781	0.738709	15.65758
907		0.657245	0.76763	15.65758	1010		0.793995	0.65613	15.65758
908		0.379121	0.93263	15.65758	1011		0.723311	0.723929	15.65758
909		0.778152	0.68659	15.65758	1012		0.629387	0.786832	15.65758
910		0.708266	0.741077	15.65758	1013		0.77112	0.669028	15.65758
911		0.741949	0.703251	15.65758	1014		0.77787	0.66907	15.65758
912		0.732645	0.709869	15.65758	1015		0.669405	0.76766	15.65758
913		0.733462	0.719083	15.65758	1016		0.705858	0.742072	15.65758

1017	0.680278	0.753871	15.65758	1120	0.71271	0.741053	15.65758
1018	0.753652	0.662044	15.65758	1121	0.590683	0.814181	15.65758
1019	0.820061	0.647687	15.65758	1122	0.717742	0.722819	15.65758
1020	0.72079	0.723806	15.65758	1123	0.692886	0.739174	15.65758
1021	0.776586	0.688046	15.65758	1124	0.630878	0.791091	15.65758
1022	0.687348	0.754433	15.65758	1125	0.735303	0.720045	15.65758
1023	0.690358	0.739867	15.65758	1126	0.631029	0.780588	15.65758
1024	0.783328	0.661857	15.65758	1127	0.722456	0.724475	15.65758
1025	0.506323	0.861537	15.65758	1128	0.531931	0.848575	15.65758
1026	0.67595	0.754128	15.65758	1129	0.70148	0.746213	15.65758
1027	0.757751	0.710844	15.65758	1130	0.763469	0.685513	15.65758
1028	0.75452	0.709793	15.65758	1131	0.639119	0.773494	15.65758
1029	0.757314	0.696604	15.65758	1132	0.772997	0.687042	15.65758
1030	0.815508	0.612907	15.65758	1133	0.828557	0.623948	15.65758
1031	0.71877	0.729066	15.65758	1134	0.695512	0.755683	15.65758
1032	0.743899	0.715105	15.65758	1135	0.742055	0.690035	15.65758
1033	0.790251	0.658635	15.65758	1136	0.6752	0.765561	15.65758
1034	0.732677	0.729678	15.65758	1137	0.813241	0.638919	15.65758
1035	0.35503	0.964937	15.65758	1138	0.800103	0.673278	15.65758
1036	0.709782	0.76099	15.65758	1139	0.778431	0.663085	15.65758
1037	0.531547	0.847224	15.65758	1140	0.665075	0.758563	15.65758
1038	0.732107	0.723587	15.65758	1141	0.239762	0.998118	15.65758
1039	0.744643	0.674368	15.65758	1142	0.665556	0.757436	15.65758
1040	0.627713	0.793194	15.65758	1143	0.700001	0.735559	15.65758
1041	0.756276	0.688384	15.65758	1144	0.678126	0.762227	15.65758
1042	0.653043	0.780371	15.65758	1145	0.747102	0.705114	15.65758
1043	0.560027	0.833088	15.65758	1146	0.803634	0.660102	15.65758
1044	0.711066	0.725508	15.65758	1147	0.783473	0.669712	15.65758
1045	0.756527	0.710687	15.65758	1148	0.747155	0.708985	15.65758
1046	0.818695	0.634769	15.65758	1149	0.725198	0.702334	15.65758
1047	0.695607	0.735414	15.65758	1150	0.685829	0.75145	15.65758
1048	0.714009	0.72878	15.65758	1151	0.502274	0.864317	15.65758
1049	0.712248	0.741944	15.65758	1152	0.782728	0.672239	15.65758
1050	0.775953	0.672263	15.65758	1153	0.72986	0.727101	15.65758
1051	0.744133	0.703175	15.65758	1154	0.773939	0.697421	15.65758
1052	0.772121	0.684686	15.65758	1155	0.687333	0.743767	15.65758
1053	0.713474	0.728495	15.65758	1156	0.707543	0.731405	15.65758
1054	0.771891	0.685924	15.65758	1157	0.845588	0.611515	15.65758
1055	0.809628	0.654636	15.65758	1158	0.710151	0.732487	15.65758
1056	0.760103	0.692118	15.65758	1159	0.641018	0.772645	15.65758
1057	0.78302	0.678274	15.65758	1160	0.661364	0.776176	15.65758
1058	0.745836	0.714558	15.65758	1161	0.808727	0.653302	15.65758
1059	0.768741	0.697168	15.65758	1162	0.766915	0.69704	15.65758
1060	0.704826	0.749205	15.65758	1163	0.686071	0.753808	15.65758
1061	0.775161	0.683603	15.65758	1164	0.599673	0.805603	15.65758
1062	0.732497	0.702145	15.65758	1165	0.794448	0.629683	15.65758
1063	0.794772	0.653777	15.65758	1166	0.802811	0.644151	15.65758
1064	0.704785	0.741416	15.65758	1167	0.651216	0.772093	15.65758
1065	0.610918	0.803309	15.65758	1168	0.795941	0.674203	15.65758
1066	0.73975	0.703612	15.65758	1169	0.72548	0.711849	15.65758
1067	0.578734	0.819566	15.65758	1170	0.739106	0.712871	15.65758
1068	0.755852	0.712753	15.65758	1171	0.730707	0.71683	15.65758
1069	0.757024	0.697733	15.65758	1172	0.698956	0.743106	15.65758
1070	0.790732	0.687048	15.65758	1173	0.809202	0.661838	15.65758
1071	0.63718	0.77523	15.65758	1174	0.821564	0.578432	15.65758
1072	0.672559	0.764661	15.65758	1175	0.632834	0.784984	15.65758
1073	0.551601	0.837156	15.65758	1176	0.577107	0.821497	15.65758
1074	0.838523	0.610499	15.65758	1177	0.707338	0.741701	15.65758
1075	0.78146	0.649677	15.65758	1178	0.715981	0.736117	15.65758
1076	0.757695	0.682712	15.65758	1179	0.764327	0.675078	15.65758
1077	0.765066	0.691627	15.65758	1180	0.807443	0.655474	15.65758
1078	0.798581	0.656941	15.65758	1181	0.681317	0.739627	15.65758
1079	0.66402	0.761724	15.65758	1182	0.73531	0.704112	15.65758
1080	0.720704	0.730526	15.65758	1183	0.66009	0.755459	15.65758
1081	0.660943	0.768078	15.65758	1184	0.740376	0.714956	15.65758
1082	0.819114	0.637775	15.65758	1185	0.776033	0.672729	15.65758
1083	0.74674	0.695437	15.65758	1186	0.740137	0.69061	15.65758
1084	0.709397	0.741257	15.65758	1187	0.63157	0.787747	15.65758
1085	0.711678	0.738512	15.65758	1188	0.754081	0.697833	15.65758
1086	0.688208	0.753062	15.65758	1189	0.74844	0.685375	15.65758
1087	0.793762	0.656493	15.65758	1190	0.727209	0.735502	15.65758
1088	0.708538	0.730728	15.65758	1191	0.656472	0.77443	15.65758
1089	0.801037	0.669775	15.65758	1192	0.796227	0.658925	15.65758
1090	0.641376	0.776633	15.65758	1193	0.772166	0.672837	15.65758
1091	0.736028	0.720062	15.65758	1194	0.715671	0.736194	15.65758
1092	0.674931	0.768255	15.65758	1195	0.52654	0.849773	15.65758
1093	0.776621	0.659614	15.65758	1196	0.732145	0.726056	15.65758
1094	0.767389	0.680831	15.65758	1197	0.705633	0.734931	15.65758
1095	0.790682	0.632699	15.65758	1198	0.768547	0.702023	15.65758
1096	0.841569	0.63514	15.65758	1199	0.71499	0.738296	15.65758
1097	0.743903	0.704644	15.65758	1200	0.764234	0.694914	15.65758
1098	0.805389	0.618343	15.65758	1201	0.673909	0.756292	15.65758
1099	0.696449	0.748044	15.65758	1202	0.682181	0.744902	15.65758
1100	0.719927	0.715891	15.65758	1203	0.774757	0.684742	15.65758
1101	0.69704	0.73399	15.65758	1204	0.680445	0.757292	15.65758
1102	0.651679	0.771676	15.65758	1205	0.69218	0.741157	15.65758
1103	0.755278	0.670244	15.65758	1206	0.76709	0.67628	15.65758
1104	0.720316	0.722533	15.65758	1207	0.736914	0.707589	15.65758
1105	0.737407	0.719694	15.65758	1208	0.708526	0.729553	15.65758
1106	0.662154	0.766654	15.65758	1209	0.708515	0.728573	15.65758
1107	0.830692	0.631771	15.65758	1210	0.740751	0.717606	15.65758
1108	0.791845	0.666042	15.65758	1211	0.623889	0.794416	15.65758
1109	0.649861	0.777237	15.65758	1212	0.807316	0.656808	15.65758
1110	0.686171	0.760505	15.65758	1213	0.762856	0.706352	15.65758
1111	0.816981	0.643317	15.65758	1214	0.712044	0.736508	15.65758
1112	0.764978	0.679219	15.65758	1215	0.588046	0.817042	15.65758
1113	0.614046	0.795592	15.65758	1216	0.755743	0.686084	15.65758
1114	0.639398	0.78214	15.65758	1217	0.757567	0.666973	15.65758
1115	0.704238	0.733455	15.65758	1218	0.278226	0.974871	15.65758
1116	0.755563	0.695235	15.65758	1219	0.725258	0.723067	15.65758
1117	0.785704	0.692678	15.65758	1220	0.70005	0.736196	15.65758
1118	0.758935	0.708937	15.65758	1221	0.58577	0.814576	15.65758
1119	0.781297	0.676508	15.65758	1222	0.723187	0.720456	15.65758

1223	0.714422	0.730269	15.65758
1224	0.577502	0.822202	15.65758
1225	0.693312	0.751261	15.65758
1226	0.791282	0.685651	15.65758
1227	0.564387	0.829423	15.65758
1228	0.747661	0.704331	15.65758
1229	0.720655	0.713909	15.65758
1230	0.662961	0.769072	15.65758
1231	0.72137	0.721816	15.65758
1232	0.686161	0.748134	15.65758
1233	0.809834	0.661821	15.65758
1234	0.76412	0.698151	15.65758
1235	0.689511	0.733263	15.65758
1236	0.792592	0.657457	15.65758
1237	0.766558	0.712442	15.65758
1238	0.761543	0.706918	15.65758
1239	0.550016	0.837194	15.65758
1240	0.730906	0.726227	15.65758
1241	0.793114	0.681477	15.65758
1242	0.784768	0.672592	15.65758
1243	0.747936	0.716881	15.65758
1244	0.725548	0.721379	15.65758
1245	0.629535	0.794369	15.65758
1246	0.839963	0.619946	15.65758
1247	0.630581	0.786691	15.65758
1248	0.802012	0.65231	15.65758
1249	0.704737	0.732707	15.65758
1250	0.684682	0.75004	15.65758
1251	0.751803	0.681922	15.65758
1252	0.727949	0.725403	15.65758
1253	0.695998	0.751598	15.65758
1254	0.484333	0.874303	15.65758
1255	0.698134	0.743205	15.65758
1256	0.714551	0.727829	15.65758
1257	0.66066	0.782367	15.65758
1258	0.785997	0.641922	15.65758
1259	0.784753	0.691787	15.65758
1260	0.779707	0.685682	15.65758
1261	0.825568	0.627843	15.65758
1262	0.72802	0.711189	15.65758
1263	0.75862	0.696339	15.65758
1264	0.747344	0.700294	15.65758
1265	0.694342	0.746211	15.65758
1266	0.860389	0.599314	15.65758
1267	0.759755	0.703841	15.65758
1268	0.642002	0.777851	15.65758
1269	0.776608	0.633207	15.65758
1270	0.744324	0.704364	15.65758
1271	0.741291	0.712387	15.65758
1272	0.744685	0.694415	15.65758
1273	0.702378	0.745417	15.65758
1274	0.779596	0.6634	15.65758
1275	0.756676	0.701942	15.65758
1276	0.677364	0.771027	15.65758
1277	0.714177	0.733026	15.65758
1278	0.722679	0.730909	15.65758
1279	0.702159	0.743194	15.65758
1280	0.74375	0.702985	15.65758
1281	0.812572	0.642327	15.65758
1282	0.720098	0.735015	15.65758
1283	0.749565	0.69603	15.65758
1284	0.75384	0.709555	15.65758
1285	0.779544	0.686506	15.65758
1286	0.585673	0.817444	15.65758
1287	0.62267	0.793432	15.65758

1288	0.75075	0.679543	15.65758
1289	0.769074	0.714154	15.65758
1290	0.672913	0.755533	15.65758
1291	0.791189	0.677605	15.65758
1292	0.687371	0.748525	15.65758
1293	0.728507	0.727564	15.65758
1294	0.712912	0.744501	15.65758
1295	0.770852	0.664634	15.65758
1296	0.722733	0.720011	15.65758
1297	0.779218	0.666609	15.65758
1298	0.647898	0.727269	15.65758
1299	0.796565	0.6778	15.65758
1300	0.777649	0.685544	15.65758
1301	0.697163	0.750899	15.65758
1302	0.723201	0.736601	15.65758
1303	0.663783	0.771957	15.65758
1304	0.79649	0.632939	15.65758
1305	0.716883	0.734674	15.65758
1306	0.826048	0.635109	15.65758
1307	0.81099	0.665067	15.65758
1308	0.721699	0.720644	15.65758
1309	0.779726	0.691522	15.65758
1310	0.707097	0.750393	15.65758
1311	0.768244	0.65827	15.65758
1312	0.693818	0.742331	15.65758
1313	0.654357	0.774034	15.65758
1314	0.731014	0.727412	15.65758
1315	0.820342	0.606148	15.65758
1316	0.719218	0.72763	15.65758
1317	0.792234	0.649942	15.65758
1318	0.607372	0.801541	15.65758
1319	0.767538	0.694009	15.65758
1320	0.672924	0.771797	15.65758
1321	0.700652	0.744471	15.65758
1322	0.704809	0.723656	15.65758
1323	0.814738	0.629158	15.65758
1324	0.790582	0.628781	15.65758
1325	0.718023	0.713256	15.65758
1326	0.783174	0.692256	15.65758
1327	0.675715	0.755211	15.65758
1328	0.659093	0.769057	15.65758
1329	0.668308	0.758882	15.65758
1330	0.669046	0.752132	15.65758
1331	0.744776	0.714642	15.65758
1332	0.670585	0.764935	15.65758
1333	0.68995	0.740489	15.65758
1334	0.607847	0.796431	15.65758
1335	0.754045	0.70841	15.65758
1336	0.611958	0.805104	15.65758
1337	0.746985	0.705477	15.65758
1338	0.753129	0.69097	15.65758
1339	0.825727	0.661501	15.65758
1340	0.697593	0.745985	15.65758
1341	0.621878	0.792016	15.65758
1342	0.760842	0.704345	15.65758
1343	0.771142	0.677164	15.65758
1344	0.775522	0.678941	15.65758
1345	0.488443	0.872785	15.65758
1346	0.687731	0.754729	15.65758
1347	0.72357	0.736731	15.65758
1348	0.756148	0.677644	15.65758
1349	0.727772	0.709451	15.65758

Table S2. Phenotypic characteristics of GTEx lung tissue donors

Feature	Number of individuals (%)	Median (range)
Sex		
Female	183 (31.7)	
Male	395 (68.3)	
Age		56 (21 - 70)
<40	73 (12.6)	
40-49	93 (16.1)	
50-59	200 (34.6)	
60-69	190 (32.9)	
>69	22 (3.8)	
Body mass index		27.7 (17.0 - 35.4)
<25	155 (26.8)	
25-30	246 (42.6)	
>30	177 (30.6)	
Race		
Caucasian	493 (85.9)	
Black/African American	70 (12.2)	
Asian	10 (1.7)	
American Indian/Alaska Native	1 (0.2)	
Smoking status		
Non-smoker	180 (32.0)	
Smoker	382 (68.0)	

Table S3. Multivariate analysis of ACE2 expression in human lung tissue

Variable	β value	S.E.	<i>t</i> value	<i>p</i> value	
CD8+ T cells	-2.719	0.584	-4.656	4.02e-06	****
NK cells resting	-3.128	0.583	-5.366	1.18e-07	****
NK cells activated	-2.281	0.704	-3.241	0.0013	**
M1 macrophages	-4.963	1.339	-3.707	0.0002	***
CD4+ T cells	0.453	0.513	0.882	0.3781	
Dendritic cells	-12.793	6.688	-1.913	0.0563	
Neutrophils	-0.398	0.469	-0.848	0.3971	
Sex = male (vs. female)	0.065	0.056	1.16	0.2466	
Age	0.004	0.002	1.799	0.0726	
BMI	-0.004	0.006	-0.556	0.5787	
Race = Caucasian (vs. non-Caucasian)	-0.096	0.073	-1.313	0.1899	
Smoking status = yes (vs. no)	-0.025	0.058	-0.433	0.6650	

Abbreviations: S.E., Standard Error.

Table S4. Meta-analysis of ACE2 mRNA and protein levels in 17 human tissues

Source data of Fig. 2f.

Source data type	Source data method	Adipose tissue	Airway epithelium	Brain	Cardiac muscle	Colorectal tissue	Endometrium	Gall bladder	Kidney	Liver	Lung	Oral mucosa/esophagus	Skin	Small intestine	Smooth muscle	Spleen	Stomach	Testis	Ref.
mRNA	NB	0	N	N	3	2	0	N	3	0	0	N	0	2	0	N	N	3	[1]
mRNA	qRT-PCR	1	1	0	2	2	1	2	2	1	1	1	0	3	1	0	1	3	[2]
mRNA	MA	2	2	2	2	2	1	N	3	2	2	N	1	3	2	N	N	3	[3]
mRNA	RNAseq	2	N	2	2	1	1	3	3	0	0	0	1	3	2	N	0	3	[4]
mRNA	RNAseq	N	N	N	N	N	N	N	N	N	N	1	N	N	N	N	N	N	[5]
mRNA	CAGE	0	N	0	1	2	0	1	1	0	0	0	N	3	0	0	N	2	[6]
Protein	MS	N	N	0	1	0	N	1	3	1	0	0	N	N	N	N	N	3	[7]
Protein	IHC	3	1	1	N	1	N	N	3	1	3	2	3	3	3	3	0	N	[8]
Protein	IHC	0	0	0	1	2	0	3	3	0	0	0	0	3	0	0	0	3	[9]
Scores (averages)																			
mRNA score		1.0	1.5	1.0	2.0	1.8	0.6	2.0	2.4	0.6	0.6	0.5	0.5	2.8	1.0	0.0	0.5	2.8	
Protein score		1.5	0.5	0.3	1.0	1.0	0.0	2.0	3.0	0.7	1.0	0.7	1.5	3.0	1.5	1.5	0.0	3.0	
Abbreviations: CAGE, cap analysis of gene expression; IHC, immunohistochemistry; MA, microarray; MS, mass spectrometry; N, not determined; NB Northern blot.																			

Supplementary References

1. Tipnis, S.R., et al., *A human homolog of angiotensin-converting enzyme. Cloning and functional expression as a captopril-insensitive carboxypeptidase.* J Biol Chem, 2000. **275**(43): p. 33238-43.
2. Harmer, D., et al., *Quantitative mRNA expression profiling of ACE 2, a novel homologue of angiotensin converting enzyme.* FEBS Lett, 2002. **532**(1-2): p. 107-10.
3. Wu, C., et al., *BioGPS: building your own mash-up of gene annotations and expression profiles.* Nucleic Acids Res, 2016. **44**(D1): p. D313-6.
4. Uhlen, M., et al., *A pathology atlas of the human cancer transcriptome.* Science, 2017. **357**(6352).
5. GTEx Consortium, *Genetic effects on gene expression across human tissues.* Nature, 2017. **550**(7675): p. 204-213.
6. FANTOM Consortium, RIKEN PMI, CLST (DGT), *A promoter-level mammalian expression atlas.* Nature, 2014. **507**(7493): p. 462-70.
7. Kim, M.S., et al., *A draft map of the human proteome.* Nature, 2014. **509**(7502): p. 575-81.
8. Hamming, I., et al., *Tissue distribution of ACE2 protein, the functional receptor for SARS coronavirus. A first step in understanding SARS pathogenesis.* J Pathol, 2004. **203**(2): p. 631-7.
9. Thul, P.J., et al., *A subcellular map of the human proteome.* Science, 2017. **356**(6340).